1702 Identification of Biomarkers of Diabetic Nephropathy Progression in Renal Transplant Patients Using Novel Chemical Imaging Approaches

VK Varma, A Susma, A Kajdacsy-Balla, S Akkina, S Setty, R Bhargava, MJ Walsh. University of Illinois at Chicago, Chicago, IL; University of Illinois at Urbana-Champaign, Urbana, IL.

Background: Kidney transplantation is the main treatment for end-stage renal disease, however close monitoring of post-transplant biopsies is required to identify subclinical complications. In high risk patients surveillance biopsies are acquired every 6 to 12 months post transplantation to examine tissue histology for complications. In this study, we focused on identifying biochemical markers associated with recurrent diabetic nepthropathy using Fourier Transform Infrared (FT-IR) spectroscopic imaging. FT-IR imaging is an emerging approach to obtain label-free images of the biochemical composition of tissue biopsies (including proteins, lipids, collagen, DNA and glycation).
Design: Initial studies identified 8 patients with no diabetic nephropathy and 8 patients with diabetic nephropathy. Serial sections were stained with PAS or imaged using FT-IR. IR spectra were extracted from the different glomerular and tubular structures and compared to identify biomarkers associated with diabetic nephropathy progression. A second study identified five transplant patients with repeat biopsies who underwent rapid recurrent diabetic nephropathy and five normal patients with no evidence of diabetic nephropathy. Biochemical information was extracted from the images to identify chemical changes associated with the progression of diabetic nephropathy.
Results: A number of biomarkers were identified that were shown to change in glomerular and tubular structures associated with increasing severity of nephropathy due to diabetes. The most robust biomarkers of disease progression were increased levels of glycation and the symmetric phosphate band in glomerular structures. These two biomarkers were also consistently found to be increasing in the cohort of patients that had multiple surveillance biopsies and underwent rapid diabetic nephropathy recurrence suggesting that these features may be predictive of early diabetic nephropathy changes.
Conclusions: FT-IR imaging is an emerging approach that can allow for novel insight into the biochemical changes associated with disease progression in transplant renal biopsies. We have identified a number of biomarkers associated with the advancement of diabetic nephropathy and that we can track the early recurrence of diabetic nephropathy in surveillance biopsies. FT-IR imaging is potentially powerful adjunct to current pathological methods allowing for the label-free and rapid identification of early markers of transplant complications.

1703 Identifying Iron Deposition in Proximal Tubules Is a Useful Method to Distinguish Sickle Cell Disease (SCD) Associated Renal Tubular Injury from Other Injury Etiologies

Y Wang, SC Wolforth, M Doshi, S Khan, MT Rooney, W Li, PL Zhang. William Beaumont Hospital, Royal Oak, MI; Detroit Medical Center, Detroit, MI.

Background: Sickle cell nephropathy (SCN) has been thought to be a vascular disorder since blood clot formation from sickle cells is considered to be the cause of renal disease. We hypothesize that sickle cells, known vulnerable for broken, may dump large amount of iron to proximal tubules and cause renal tubular injury, thus partially contributing to renal failure seen in sickle cell nephropathy. We compared iron stains in 3 cases with SCD and 29 controls.
Design: Three biopsies from patients with SCD (one native and two transplant biopsies) were stained for iron using conventional Prussian blue method. The proximal tubules were evaluated for iron staining (0 to 3+) and correlated with clinical scenarios. Controls include 12 IgA nephropathy, 13 thrombotic microangiopathy (TMA) and 4 "pure" acute tubular necrosis (ATN) cases were also stained for iron.
Results: All controls showed negative or minimal iron staining in proximal tubules, except two TMA with 2+ iron staining in proximal tubules. The first native biopsy with SCD showed membranoproliferative pattern of glomerulopathy and 3+ iron staining in proximal tubules, consistent with a SCN. The second patient, status post renal transplant 2 years ago, developed acute renal failure, and his renal biopsy was found to have acute tubular injury (ATI). Diffusely increased iron staining (2+) in proximal tubules was present, thus the ATI was most likely resulted from iron toxicity to proximal tubules, and EM confirmed aggregated sickled RBC in glomeruli, indicating a recurrent SCN. The third patient, status post renal transplant 4 years ago, developed acute renal failure and positive donor specific antibody. His renal biopsy revealed 1a acute cellular rejection, diffuse positive C4d in peritubular capillaries and thrombotic microangiopathy (TMA). The iron staining was focally and weakly present, implying that the TMA was most likely associated with the acute antibody mediated rejection (AAMR, type 2) rather than recurrent SCN.
Conclusions: Our data indicate that iron staining is a non-expensive but effective method in distinguishing SCD associated renal injury from other etiologies, supporting the view that iron overloading in proximal tubules could be a cause of ATI.

1704 Hic-5 and Glomerular Senescence in Chronic Proteinuric Glomerulopathies

A Weins, P Mundel. Brigham and Women's Hospital, Boston, MA; Massachusetts General Hospital, Boston, MA.

Background: Diffuse diabetic glomerulosclerosis (DDG) and Primary Focal Segmental Glomerulosclerosis (FSGS) are patterns of glomerular injury clinically characterized by slow progression and proteinuria. To date little is known about molecular mechanisms involved in the evolution from minimal proteinuria and mild podocyte injury to nephron loss. This study explores a role of the focal adhesion protein hic-5 in this process by focusing on hic-5 expression in glomerular mesangial and epithelial cells. The findings build on our recently published results on the pathogenesis of progressive glomerular lesions.
Design: We performed immunohistochemical analysis of archived kidney biopsies from patients with DDG and FSGS, and control cases (including Minimal Change Disease, IgA Nephropathy, Vascular Disease and Acute Tubular Injury). In addition, mouse models of chronic glomerular disease (AT1R transgenic rats, murine ADR nephropathy), mouse models of acute glomerular disease (Protamine Sulfate perfusion and injection of Nephrotoxic Serum) and conditionally immortalized podocytes were used to explore the role of hic-5 in chronic versus acute glomerular injury.
Results: While hic-5 expression is limited to vascular smooth muscle cells in control cases, glomeruli in DDG and FSGS show specific and robust up-regulation of hic-5 in mesangial and in scattered glomerular epithelial cells. In addition, the same samples also reveal features of cellular senescence in occasional glomerular epithelial but not mesangial cells, as confirmed by focal low-level expression of p53 and positive SA-beta-galactosidase staining. Conditionally immortalized podocytes with up-regulation of hic-5 at focal adhesions show increased adhesiveness to the ECM and concomitant features of cellular senescence. Glomeruli of AT1R tg rats and of mice with ADR nephropathy, both models of progressive glomerular injury, also reveal substantial up-regulation of hic-5 compared to their wild type littermates. In contrast, hic-5-/- mice show neither protection nor worsening of acute podocyte FPE or proteinuria compared to wild type littermates after perfusion with protamine sulfate or injection of Nephrotoxic Serum.
Conclusions: These findings suggest a link between hic-5 and glomerular senescence in progressive glomerular injury. Understanding if adhesion-dependent induction of senescence may promote intraglomerular cross talk, and how it participates in accelerating or decelerating disease progression is the focus of further studies, and may help to identify novel and specific therapeutic targets.

1705 Conditional PAI-1 Knock-Out Protects Against Podocyte Injury in Mice

J Yang, H-C Yang, AB Fogo. Vanderbilt University Medical Center, Nashville, TN.

Background: Plasminogen activator inhibitor-1 (PAI-1) prevents matrix degradation by inhibiting plasmin formation and regulates cell function by the vitronectin pathway. We previously showed that systemic PAI-1 knockout mice were resistant to glomerulosclerosis after 5/6 nephrectomy. In vitro, PAI-1 deficient podocytes had reduced apoptosis and preserved cytoskeleton after injury compared to wild type. In this study, we therefore investigated whether conditional podocyte PAI-1 knock-out could protect against glomerulosclerosis in a primary podocyte injury model.
Design: By mating PAI-1^{loxp}/Teto-Podocin Cr^{+} mouse with PAI-1^{loxp}/Nep25 mouse, we generated conditional PAI-1 knock-out mice (KO; PAI-1$^{loxp/loxp}$/Teto-Podocin Cre^{+}/Nep25, n=7) and wild type mice (WT; PAI-1$^{loxp/loxp}$/Teto-Podocin Cre^{-}/ Nep25, n=8). These Nep25 positive mice expressed human CD25 on podocytes, and thus, podocyte injury and a primary FSGS can be induced by injecting the LMB2 toxin which binds CD25. On Day -7, doxycycline (2mg/ml) was added to drinking water to induce podocyte knock-out of PAI-1. On Day 0, LMB-2 (8 ng/g BW, I.V.) was given. Mice were sacrificed and kidneys were harvested on Day 10.
Results: Both groups showed similar edema, reflected by increased body weight. KO had a trend to increased blood pressure vs WT (change vs baseline KO 18.8±7.0 *vs.* WT 1.5±4.9%, p=0.061). Proteinuria was similar between groups (urine protein:creatinine ratio WT 463.2±72.1, *vs.* KO 496.9±49.6mg/ug, pNS). Podocyte injury was numerically increased in WT (semi-quantitative score, 0-4, WT 2.78±0.11, *vs.* KO 2.26±0.27, p=0.084). Synaptopodin expression, a marker of differentiated podocytes, was higher in KO *vs.* WT (glomerular positive area %, KO 3.82±0.87, *vs.* WT 1.98±0.23%, p<0.05). The glomerulosclerosis score and % collagen IV area in glomerulus were not different between groups (WT 12.80±1.19, vs. KO 14.47±0.90%, pNS).
Conclusions: Knock-out of PAI-1 in podocytes results in better maintenance of podocytes after injury, but does not appear to be sufficient to prevent glomerulosclerosis or matrix accumulation in vivo. Taken together with previous systemic PAI-1$^{-/-}$ data, these findings support that additional glomerular or infiltrating cell PAI-1 is crucial for perpetuating sclerosis after injury.

Liver

1706 Loss of ARID1A Expression Is a Late Stage Event in Tumor Progression of Hepatocellular Carcinoma

H Abe, A Hayashi, A Kunita, J Shibahara, M Fukayama. the University of Tokyo Hospital, Tokyo, Japan; Graduate School of Medicine, The University of Tokyo, Tokyo, Japan.

Background: AT-rich interactive domain 1A (ARID1A) is a subunit of Switch/Sucrose non-fermentable (SWI/SNF) chromatin remodeling complex. Frequent mutation and loss of protein expression were reported in various carcinomas such as ovarian clear cell carcinoma and Epstein-Barr virus associated gastric carcinoma. Recently, genome-wide whole exome sequencing revealed frequent mutation of ARID1A in hepatocellular carcinoma. However, the clinicopathological significance and the role in carcinogenesis were unknown.
Design: In this study, immunohistochemistry of ARID1A was performed in tissue microarray of 290 hepatocellular carcinomas, and clinicopathological significance was analyzed. In addition, distribution of ARID1A-lost carcinoma cells within the tumor was examined by immunohistochemistry of whole sections. Expression of ARID1A in 19 dysplastic nodules was also examined.
Results: Eleven (3.8%) of 290 cases showed loss of ARID1A expression. Loss of ARID1A expression has no significant correlation with age, sex, HBV or HCV infection, cirrhosis, TNM stage, tumor size, histology, number of tumors, vascular invasion, nor survival. Both beta-catenin and p53 expression showed no significant association with ARID1A. By immunohistochemistry of the whole sections, four (36%) of 11 cases

with loss of ARID1A showed localized negative area adjacent to positive area within the tumor. All of the 11 cases were negative for EBER-ISH. None of the dysplastic nodules showed loss of ARID1A (0/19).
Conclusions: Loss of ARID1A expression is a late stage event in the cancer progression and occurs in clones within the tumor. The role of ARID1A in hepatocellular carcinoma is different from that of ovarian clear cell carcinoma or Epstein-Barr virus associated gastric carcinoma, in which loss of ARID1A was reported to be an early change in carcinogenesis.

1707 AKR1C3 as a Marker to Distinguish Well Differentiated HCC from Benign Hepatic Lesions

AC Annan, SW Lindley, MM Yeh, V Jayaprakash, K-MA Fung. University of Oklahoma Health Sciences Center, Oklahoma City, OK; University of Washington, Seattle, WA; Roswell Park Cancer Institute, Buffalo, NY.
Background: Aldo-keto reductase family 1 member C3 (AKR1C3) is an enzyme with multiple functions including working as a steroid dehydrogenase. We evaluated the expression of AKR1C3 in hepatitis, hepatic adenoma, cirrhosis, focal nodular hyperplasia (FNH), hepatocellular carcinoma (HCC) and metastatic HCC.
Design: Formalin-fixed, paraffin embedded sections (2 cases of hepatitis, 6 cases of hepatic adenoma, 8 cases of cirrhosis, 6 cases of FNH, 22 cases of HCC, and 3 cases of metastatic HCC) were immunostained for AKR1C3. Immunoreactivities were scored as 0 (no staining), 1+ (focal mild staining), 2+ (diffuse mild/focal strong staining), 3+ (diffuse strong staining). The cases were divided into cohorts of cancer group (HCC and metastatic HCC) and non-cancer group (hepatitis, hepatic adenoma, cirrhosis, and FNH) with appropriate controls.
Results: In the cancer cohort, we demonstrated a 2+ or 3+ staining in 20/25 cases (80%). In the non-cancer cohort, 2+ staining was demonstrated in 2 out of 6 adenoma (33.3%) and 1 out of 6 FNH (16.7%) with no 3+ staining demonstrated. Positive immunoreactivities were also demonstrated in other non-cancer cases. With all cases considered, Fisher's exact test was performed for staining pattern of $\geq$2+($p=0.008$) and 3+ ($p<0.001$). The sensitivity of the $\geq$2+ staining pattern was 80% with a negative predictive value of 72% to exclude HCC. With the 3+ staining pattern the sensitivity dropped to 52%, but the specificity was 96% and had a positive predictive value of 93% for HCC.

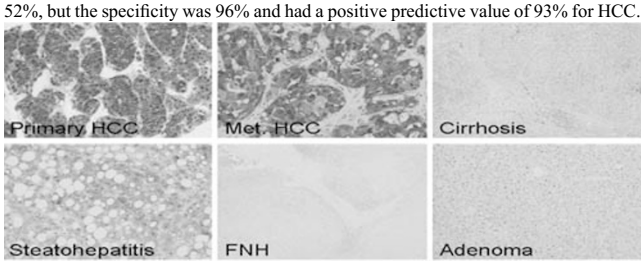

Conclusions: Histologic differentiation of an adenoma from a well-differentiated HCC can be challenging. With a strong specificity (96%) and positive predictive value (93%) for a 3+ scoring pattern for HCC, AKR1C3 immunohistochemistry can be an important adjunct to differentiate well-differentiated HCC from benign mimics.

1708 Morphology, Tumor Genetics, and Outcomes in Five Cases of Biliary Adenofibroma

T Arnason, D Borger, C Corless, C Hagen, J Iafrate, H Sapp, WM Tsui, IR Wanless, T Zuluaga Toro, GY Lauwers. Queen Elizabeth II HSC, Halifax, NS, Canada; Massachusetts General Hospital, Boston, MA; Oregon Health & Science University, Portland, OR; Caritas Medical Center, Kowloon, Hong Kong; University of Florida, Gainesville, FL.
Background: Biliary adenofibroma is a rare primary hepatic neoplasm, recognized in the 2010 WHO Classification of liver tumors. However, there are less than a dozen case reports of this entity. Here we present the first series of patients with biliary adenofibroma, including extended follow up of 2 previously reported cases and 3 novel cases.
Design: Slides and clinical history were reviewed. Tumor DNA was extracted and analyzed for point mutations in *AKT1, APC, BRAF, CTNNB1, IDH1, KIT, KRAS, MAP2K1, NRAS, PIK3CA,* and *PTEN* by multiplex PCR in 4 cases and for copy number alterations by array comparative genomic hybridization (aCGH) in 2 cases.
Results: The 4 females and 1 male presented at a mean age of 64 years (range 47-83 years). Four patients had a single tumor and 1 patient had 3 tumors. The mean diameter of the largest tumor was 10.4 cm (range 7-16cm). Morphologically, the tumors were similar, with tubular and cystic structures lined by cuboidal to columnar epithelium (with CK7, CK19, and CA19-9 expression) embedded in a fibrous stroma (with no mesenchymal marker expression except vimentin). 4 cases showed areas where the epithelium had pencillate, hyperchromatic nuclei. Multiplex PCR did not identify any mutations in 4 tumors tested. Both tumors tested by aCGH showed significant numbers of chromosomal copy number alterations. One tumor showed large region gains of 1q and loss of 1p, 2p, 3q, 6q, 8p, 11p, 12q, 14, and 16q. A second tumor had gain of 1p and loss of 11q, 22q, and Xq. This tumor also demonstrated two focal amplifications, one involving the *CyclinD1* (*CCND1*) gene and the other the *HER2* (*ERBB2*) gene. 3 patients had complete resection with no recurrence at 20 years, 3 years, and 3 months follow up. The 4th patient was alive after 14 months with no resection. The 5th patient had incomplete resection and had recurrence 6 years later. She underwent hepatectomy with liver transplant and died of transplant complications. No patient had metastatic disease.
Conclusions: Biliary adenofibromas have a distinct histomorphology. The presence of multiple clonal cytogenetic alterations supports that they are neoplastic lesions. Amplifications of *CCND1* and *ERBB2* are not typical of benign neoplasms, and suggest that these tumors may have the ability to behave aggressively. However, the clinical outcomes in these patients suggest the neoplasms are slowly progressive with low (if any) metastatic potential.

1709 Morphologic Features to Distinguish Early Chronic Rejection from Recurrent Hepatitis C in Liver Allografts

BD Buelow, RM Gill. UCSF, San Francisco, CA.
Background: Hepatitis C (HCV) represents a major cause of chronic liver disease leading to orthotopic liver transplantation. Re-infection of the allograft with HCV is common and management represents a balancing act between sufficient immunosuppression to prevent acute and/or chronic rejection and adequate immune function to prevent virus-induced injury. The gold standard for guiding these treatment decisions is liver biopsy. However, many cases arise in which distinguishing early chronic rejection from recurrent viral infection is difficult, and no criteria have been established to firmly delineate these two processes. In this study, we hypothesize that morphologic changes can identify early chronic rejection distinct from recurrent viral infection.
Design: We searched the UCSF CoPath database for recent cases of recurrent HCV, chronic rejection in the setting of HCV, and chronic rejection in the absence of HCV. No cases with crossover between groups or cases of fibrosing cholestatic HCV were included. From this pool 10 cases of "pure" recurrent HCV (RH), 10 cases of "pure" chronic rejection (CR), and 10 test cases with a differential diagnosis including recurrent HCV and early chronic rejection (TC) were matched for age/gender and then evaluated in a blinded fashion by two independent pathologists for evidence of recurrent HCV and/or early chronic rejection. Results were analyzed by Fisher's exact test for association of each feature with CR versus RH.
Results: Loss of bile ducts from portal tracts was strongly associated with CR (Bile duct/Portal tract ratio [BD/PT] = 0.53 $\pm$ 0.17) compared to RH (BD/PT = 0.95 $\pm$ 0.04). The presence of interface activity ($p=0.018$) and acidophil bodies ($p=0.047$) were associated with RH, while bile duct damage ($p=0.000$), cholestasis ($p=0.001$) and hepatocyte swelling ($p=0.018$) were strongly associated with CR. The presence of parenchymal/portal inflammation, ductular reaction, eosinophils, mixed inflammation, endothelialitis, and steatosis were not associated with either CR or RH, and thus are not useful in re-classifying TC cases.
Conclusions: The BD/PT ratio, interface activity, acidophil bodies, bile duct damage, cholestasis, and hepatocyte swelling are the most useful morphologic features to distinguish early CR from RH. Studies on immunohistochemical adjuncts to these features are ongoing, to further aid in the diagnosis of difficult cases. Our work is the largest case series to date specifically addressing this difficult differential diagnosis and provides new tools for distinguishing early chronic rejection from recurrent hepatitis C in liver allografts.

1710 An Integrated Molecular Characterization Correlates with the Progression of Hepatocellular Carcinoma

G Carrasco-Avino, JT Dudley, SC Ward. Mount Sinai School of Medicine, New York, NY.
Background: Translational hepatocellular carcinoma (HCC) research incorporates clinical data and molecular genomics analytical methods. HCC genetics and molecular pathways describing differences with non-tumoral tissue and different tumor stages have been published. Additional comparative and integrative approaches of gene profiling, biological functions and canonical pathways (CPs) may facilitate discovery of novel biomarkers. We performed a software-based analysis of public gene expression datasets for biological functions in HCC development from normal liver (NL) through cirrhosis to very advanced HCC (VAHCC).
Design: In Silico analysis of HCC Public GEO datasets (GSE6764; HG-U133_Plus_2) from 35 HCC (8 very early, 10 early, 7 advanced and 10 VAHCC), 10 NL, 13 cirrhosis, and 10 low and 7 high grade dysplastic nodules. Data were normalized by BrB Array Tools v4.3.2. Gene expression of above groups were compared by one-way ANOVA ($p<0.01$; adjusted Bonferroni) and Hierarchical Clustering Analysis (HCA; average linkage, Euclidean distance) based on significant genes only (MeV v4.9). Significant genes were analyzed using Ingenuity Pathway Analysis (IPA).
Results: One-way ANOVA identified 5029 significantly different expressed genes across the comparison groups. HCA grouped HCC and non-cancer tissues and their subgroups; the genes were integrated and analyzed by IPA showing a linear progression from NL to VAHCC in biological functions from Cancer to Hepatic System Disease, toxicity functions and CPs, such as the progressive activation of G2/M DNA Damage Checkpoint Regulation ($p< .001$).

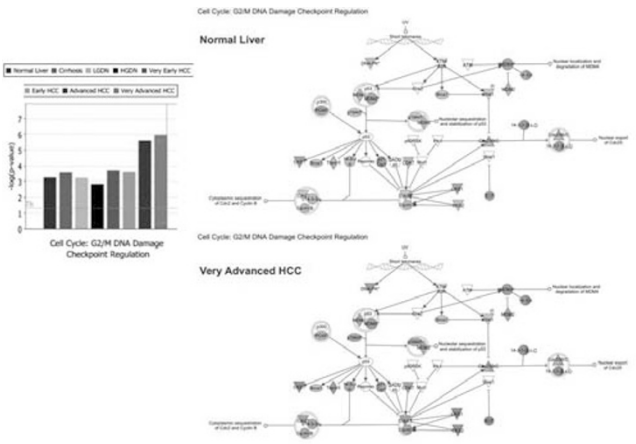

Conclusions: HCC and non-cancer tissues had different specific gene expression profiles. IPA showed activation of several biological functions, identifying interactions in CPs from NL through to VAHCC at the molecular level. Further study of these gene interactions may help identify new predictive and prognostic biomarkers and therapeutic targets. We illustrate the value of these analytical approaches in cancer research as an avenue of expansion of pathology as an academic discipline with contributions from genomics and bioinformatics.

1711 Pure Globular Hepatic Amyloid Is Highly Specific for LECT2 Amyloidosis

VS Chandan, SS Shah, DM Lam-Himlin, MS Torbenson, T-T Wu. Mayo Clinic, Rochester, MN; Mayo Clinic, Scottsdale, AZ.

Background: Liver involvement in amyloidosis typically shows linear deposition in the blood vessels or perisinusoidal space or both. Amyloid deposition in the form of globular inclusion-like bodies (globular hepatic amyloid, GHA) is rare and its significance is unclear. Recently, leukocyte chemotactic factor 2 (LECT2) associated amyloidosis involving the liver has been described as showing a globular pattern. The goal of our study was to study the prevalence & significance of GHA.

Design: 65 consecutive cases of hepatic amyloidosis (confirmed by Congo red stain; 45 needle biopsies, 13 liver explants, 6 wedge biopsies, 1 lobectomy) diagnosed between 1998 and 2013 were retrieved from our institutional files. Each case was reviewed for type of amyloid (by immunohistochemistry and/or mass spectrometry (MS)), pattern (linear or globular), and distribution (vascular, perisinusoidal or stromal in portal area). LECT2 immunostain was performed on cases with available material (25 cases).

Results: 37 (57%) were men & 28 (43%) were women with median age of 60 years (range 36-84 y). The amyloid was AL-type in 40 cases (62%), ATTR in 15 cases (23%), 3 cases each of AFib 3 (4.5%) and AA (4.5%), & 2 cases each of AApoA1 (3%) and LECT2 (3%). Of the 65 cases only 5 (7.7%) showed GHA, out of which only 2 (3%) showed pure GHA deposits. These 2 cases of pure GHA showed a prominent perivenular distribution around terminal hepatic venules and portal vein branches, perisinusoidal distribution around periportal and zone 3 regions, as well as portal stromal deposition. Both these cases were positive for LECT2 immunostain and in 1 of them MS was also performed which showed LECT2 amyloid. Other 3 (4.7%) cases showed mixed, linear (perisusoidal & vascular) and GHA (within the perisinusoidal space but no portal stromal or perivenular distribution) deposits. All these 3 cases were AL-type (confirmed on immunohistochemistry and MS) and all were negative by LECT2 immunostain. GHA was intrahepatic and in the reticuloendothelial cells in all 5 cases (100%). LECT2 immunostain was negative in the remaining 20 cases (9 AL, 5 ATTR, 3 AA, 2 AFib, 1AApoA1). Review of 2 additional cases of LECT-2 amyloid (positive on the LECT2 immunostain) from our recent consultation files also showed only pure GHA deposits with a similar pattern of distribution described above.

Conclusions: GHA is rare within the liver (7.7%). When present in its pure form, it appears to be highly specific for LECT2 associated amyloidosis. LECT2 immunostain is a very sensitive and specific tool for confirming this amyloid type.

1712 Detection of HCV antigen in Paraffin-Embedded Liver Transplant Biopsy Specimen by Immunohistochemistry and Correlation with Laboratory Findings

M Cho, CH Hajdu, R Xu. New York University, New York, NY.

Background: Recurrent hepatitis C (HepC) and acute cellular rejection (ACR) are two major problems for Hepatitis C virus (HCV) positive patients after liver transplantation. The aim of this study is to analyze the utility of two anti-HCV antibodies in detection of HCV antigens in paraffin embedded liver transplant biopsy from HCV+ patients, and to correlate HCV antigen expression with clinical/laboratory findings.

Design: Liver allograft biopsies of 35 HCV+ patients (man:woman= 26:9) were randomly retrieved from the departmental archives from 2005 to 2012. The histological diagnosis includes 19 recurrent HepC, 7 ACR, 9 mixed HepC and ACR at times of biopsy. The laboratory data pertinent to the reason of biopsy were collected from the LIS system. Immunohistochemistry was performed using two antibodies against HCV non-structural region of HCV (NS3-NS4) and NS5B RNA-dependent RNA polymerase to detect the expression of HCV antigen. The stain result was defined as negative (no stain) and positive (cytoplasmic staining pattern). Fisher exact test and Chi square analyses were performed when appropriate.

Results: Two antibodies, NS5B and NS3-NS4, detected HCV antigen in 7 (25%) and 18 (51%) cases, respectively. Thus, NS3-NS4 was chosen for further study. 7 of 19 (37%) HCV recurrence cases, 7 of 7 (100%) ACR and 4 of 9 (44%) mixed cases were positive for HCV by immunostain. The rate of positive HCV antigen detection was higher in ACR cases than HCV recurrence ($p<0.01$) and mixed cases ($p<0.05$), whereas no difference existed between the recurrence and the mixed cases ($p>0.05$). The positive HCV antigen detection rate was correlated with high serum viral load (>100 thousands units) (13/16, or 45%) than lower (<100 thousands units) (3/29, or 10%) ($p<0.05$), and with high total bilirubin (median 4 and 1.2 units in stain+ and - cases, respectively, $p<0.05$). There was no statistical difference between the detection of HCV antigen and serum levels of alanine aminotransferase, aspartate aminotransferase and alkaline phosphatase ($p>0.05$).

Conclusions: The detection of HCV antigen by immunohistochemistry in allograft liver biopsies positively correlates with high viral load and total bilirubin value. Although a paradoxical higher detection rate of HCV antigen in ACR cases is an interesting finding, the value of immunohistochemical analysis to distinguish between ACR and recurrent HepC needs further investigation.

1713 Retinoid and Carotenoid Depletion in Hepatitis C: Fibrosis Staging in Relation to Biomarkers of Serum Antioxidant Status, Insulin Resistance, and Oxidative Stress

B Chung, E Enk Rueter, S Colter, D Jensen, G Guzman, R van Breemen, P Gann. University of Illinois at Chicago, Chicago, IL; Loyola University Health System, Maywood, IL; The University of Chicago, Chicago, IL.

Background: Fibrosis and cirrhosis are risk factors for hepatocellular carcinoma in hepatitis C. Chronic inflammation and oxidative stress may activate myofibroblast transformation in Ito cells resulting in loss of vitamin A storage and increased collagen synthesis. Lower serum retinol and carotenoid levels, in addition to causing increased genetic damage, could accelerate fibrosis and hepatocarcinogenesis through promoting insulin resistance. Retinoid and carotenoid deficiencies thus may represent a modifiable risk factor for fibrosis progression at pre-cirrhotic stages through dietary supplementation or glucose control.

Design: 68 hepatitis C patients scheduled for staging biopsy and 12 healthy controls were consecutively enrolled and frequency matched by age, gender, and insurance type. Medical, lifestyle, and anthropometric data were obtained via questionnaire and medical records, and a fasting blood sample was drawn. Liver core biopsies were staged for fibrosis by H&E and Masson's trichrome stain. Serum was assayed for retinoid and carotenoid levels, HOMA index (insulin resistance) and high sensitivity CRP. Biomarkers were compared across well-defined subgroups of controls and hepatitis C patients with fibrosis stage 0, I/II, and III/Child-Pugh A. Mean values, 95% confidence intervals and P values from independent sample t-tests were calculated using MS Excel.

Results: Mean serum concentrations of retinol and lycopene demonstrated a downward trend with increasing severity of disease and statistically significant decreases between each fibrosis stage versus controls (retinol p-values: fibrosis 0, 0.046; fibrosis I/II, 0.014; fibrosis III/Child-Pugh A, 0.011; lycopene p-values: fibrosis 0, 0.007; fibrosis I/II, 0.0006; fibrosis III/Child-Pugh A, 0.004). There were no statistically significant differences in mean body-mass index or HOMA between subgroups. However, a statistically non-significant downward trend in hs-CRP was observed with increasing disease severity.

Conclusions: Serum retinol and lycopene levels are decreased during the early stages of fibrosis in hepatitis C. These changes are not associated with insulin resistance while CRP may decline due to reduced hepatic synthesis, losing its utility as an inflammation biomarker. Further analyses of liver tissue antioxidant levels and immunohistochemical biomarkers will be required before feasible and safe intervention studies with antioxidant supplementation can be designed.

1714 Steatohepatitis-Like Changes in Focal Nodular Hyperplasia, a Finding Not to Be Confused with Steatohepatitic Variant of Hepatocellular Carcinoma

K Deniz, R Moreira, M Yeh, L Ferrell. Erciyes University, Kayseri, Turkey; Mayo Clinic, Rochester, MN; University of Washington, Seattle, WA; University of California, San Francisco, CA.

Background: Steatohepatitis-like change (SLC) has not been described in focal nodular hyperplasia (FNH). This study was initiated after SLC was noted in FNH by one of the authors in the setting of consultation from a referring pathologist who was considering the diagnosis of steatohepatitic variant of hepatocellular carcinoma (HCC). This problem can be compounded if seen in FNH with widened cell plates >3 or hepatocyte small acinar change/rosettes, other features that can also be seen in HCC. This study examines steatotic FNHs for the frequency of SLC, especially in the setting of FNH with rosettes and/or widened cell plates.

Design: 35 resection specimens of steatotic FNH from 3 sites were evaluated for degree of steatosis, background liver steatosis, ductular reaction, and lymphocytic infiltrate (all graded on a scale of 0-3), as well as presence of thick fibrous bands, thick-walled (dysplastic) vessels, ballooned hepatocytes, Mallory-Denk bodies (MB), dilated sinusoids, hepatocyte rosettes, and thick hepatic plates (>3 cells).

Results:

Table 1

	Absent	Mild	Moderate	Marked
Fat	0	26	3	6
Background fat*	14	11	5	1
Ductular reaction	0	5	14	16
Lymphocyte infiltrate	1	15	14	5

*background liver not sufficient to evaluate in 4 cases

Table 2

	Absent	Present
Ballooned hepatocytes	15	20
Mallory-Denk bodies	21	14
Fibrous bands	2	33
Thick-walled vessels	5	30
Hepatocyte rosettes/acini	13	22
Thick plates	29	6

Steatosis was distributed along fibrous septa as well as diffusely throughout the FNH. SLC of MB and ballooning were focally present in 57%. Neutrophilic infiltrates were not a reliable parameter for SLC because of so-called "surgical" hepatitis, which is often seen in liver resections.Thick plates>3 cells were noted but not common; rosettes were common. Most of the lesions showed thick fibrous bands and thick-walled vessels.

Conclusions: More than half of fatty FNH examined for this study had features of at least focal SLC. This finding should not be confused with steatohepatitic variant of HCC. Widened cell plates >3 and hepatocyte rosettes as representative of other overlapping features with HCC were also present. Common typical features of FNH including thick-walled vessels, ductular reaction and thick fibrous bands are helpful for discrimination of FNH from HCC.

1715 Expression of Glutamine Synthethase in Cirrhosis and Potential Use as a Marker for Early Liver Cancer Diagnosis

LV Duckworth, T Zuluaga Toro, X Lu, C Liu. University of Florida, Gainesville, FL.

Background: Glutamine synthetase (GS) is a target gene of β-catenin, and its overexpression is associated with activation of the Wnt/β-catenin pathway, implicated in the pathogenesis of hepatocellular carcinoma (HCC). While GS is expressed in centrilobular hepatocytes in normal liver, diffuse staining for GS has been reported in 86% of moderate- to poorly-differentiated HCCs, 59% of well-differentiated HCCs, and 14% of high-grade dysplastic nodules. The aim of our study was to evaluate expression and distribution of GS in cirrhotic livers of different etiologies to determine if altered GS expression pattern could be used as an early diagnostic marker for liver dysplasia/HCC.

Design: 100 liver explants were identified through retrospective review over the last 10 years. Five groups were identified as follows: (1) non-cirrhotic liver (control group); (2) viral cirrhosis (HCV or HBV) without HCC; (3) viral cirrhosis with HCC; (4) biliary cirrhosis; and (5) cirrhosis due to fatty liver disease. GS immunohistochemistry was performed on 89 non-tumor sections and semi-quantitative analysis was performed as follows: intensity of expression (0, 1+, 2+, 3+) and percentage of positive hepatocytes with cytoplasmic staining were multiplied to obtain a Total Histo score. Distribution of expression was recorded as either portal, perivenular, or diffuse and number of cell layers staining in each area was recorded.

Results: There was a significant difference in GS expression between non-cirrhotic (66.0) and cirrhotic liver (105.0) (p=0.0152). GS expression was highest in cases of biliary cirrhosis and fatty liver disease, and the latter showed a more diffuse, characteristic "geographic" pattern of expression. Portal expression of GS was seen solely in cirrhotic livers. In addition, a significant increase in portal cell layer staining was seen in cirrhotic livers with HCC (3.8) versus cirrhotic livers without HCC (2.0) (p=0.0214).

Conclusions: Our study confirms altered expression of GS from a centrilobular region in normal liver to periportal and/or diffuse expression in cirrhotic liver. In addition, increased GS portal cell layer staining in cirrhotic livers may be indicative of early progression to HCC.

Table 1. Expression and Distribution of GS staining

	Total Histo Score	Portal Cell Layers	Venous Cell Layers
Non-cirrhotic (n=20)	66.0	0	3.9
Viral cirrhosis without tumor (n=15)	63.0	1.5	1.3
Viral cirrhosis with HCC (n=16)	85.3	3.8	1.6
Biliary cirrhosis (n=18)	144.7	2.0	1.6
Fatty liver disease with cirrhosis (n=20)	116.5	2.3	0.7
	p=0.0005 (Kruskal-Wallis test)	p< 0.0001	p< 0.0001

1716 Hepatic Copper Deposition and Local Ischemia in Liver Biopsies without Cirrhosis or Chronic Biliary Disease

EE Ely, A Godambe, G Chen. St. Louis University, St. Louis, MO; Ameripath Indiana, Indianapolis, IN.

Background: Hepatic copper deposition is well described in chronic biliary diseases, cirrhosis, and Wilson disease and is rarely noted outside these settings. In fact, copper deposition is considered a key feature of chronic cholestasis and a marker of chronic biliary disease. We have noticed significant copper deposition in noncirrhotic biopsies without features of chronic biliary diseases.

Design: All liver biopsies performed from June 2012 to June 2013 were screened for copper deposition with PAS-D. Copper deposition was confirmed by Rhodamine stain for copper and graded using a semiquantitative scale (subtle 1+ to marked 4+). The prevalence of increased copper in liver biopsies was determined, excluding cases of Wilson's or biliary disease and well-established cirrhosis. Morphologic findings were categorized and possible mechanisms for copper deposition are proposed.

Results: Eleven liver biopsies had increased copper deposition with a prevalence of 1%. There was no gender predilection (6 men and 5 women) and patients were 32-70 years old. Nine were biopsies of native livers and two were of allografts. Both allograft biopsies showed evidence of recurrent hepatitis C virus (HCV) with concurrent steatohepatitis. Diagnoses for the nine native liver biopsies included HCV (2), HCV with steatosis (1), steatohepatitis (3), Budd-Chiari (1), hepatocellular carcinoma with intratumoral copper deposition (1), and hepatoportal sclerosis (1). Copper deposition varied from 1+ to 4+ with the majority being 3+ to 4+. In biopsies with more advanced fibrosis, the copper deposition was in a periportal/periseptal location as previously described. In biopsies without portal fibrosis, copper was in zone 3 or occurred in areas where a vascular lesion or dense perisinusoidal fibrosis was present. The commonality of the eleven biopsies was vascular abnormality and/or altered microcirculation with perisinusoidal fibrosis.

Conclusions: We observed copper deposition in both native and allograft liver biopsies. These biopsies did not have well-established cirrhosis and biliary abnormalities, changes recognized to be associated with increased hepatic copper. We found that increased copper was associated with vascular abnormalities and/or perisinusoidal fibrosis. The mechanism for copper deposition is unclear. The presence of vascular abnormality and perisinusoidal fibrosis in association with copper deposition suggests that local ischemia or compromise in microcirculation may play a role in the disturbance of copper excretion.

1717 The Value of HCV Detection in Biopsy Specimens of HCV-Infected Patients with Elevated Transaminases after Liver Transplantation

JM Everett, EW Dalton, J-J Pan, A Patel, MB Fallon, KJ Dasher, MJ Hobeika, VI Machicao, M Younes. University of Texas Medical School at Houston and Memorial Hermann Hospital-TMC, Houston, TX; MRC - University of Glasgow Centre for Virus Research, Glasgow, United Kingdom.

Background: The histopathological distinction between acute cellular rejection (ACR) and recurrent hepatitis C virus (HCV) in liver biopsy specimens after liver transplantation (LT) can be difficult. The aim of our study was to determine whether immunohistochemical staining for HCV (HCV-IHC) is useful in such setting.

Design: Sections of 64 formalin fixed and paraffin embedded liver needle biopsy specimens from HCV-infected LT recipients obtained for evaluation of elevated transaminases were stained for HCV glycoprotein E2 using the monoclonal antibody AP33 and the immunoperoxidase method. Stained slides were evaluated for the location, extent, and intensity of the staining without knowledge of any pathologic or clinical data. Response to treatment was correlated with the results of HCV-IHC using two-tailed Fisher's exact test, with p<0.05 considered significant.

Results: Seventeen (27%) of the 64 biopsies showed positive HCV staining in hepatocyte cytoplasm and 47 (73%) were completely negative. For the 17 HCV-IHC-positive cases, the original pathology diagnosis was recurrent HCV in 8 (47%), indeterminate in 2 (12%), ACR in 2 (12%), features of both recurrent HCV and ACR in 2 (12%), and neither HCV or ACR in 3 (18%). Four of the HCV-IHC positive cases received antiviral therapy and all (100%) had positive response; by contrast only 3 of the 13 (23%) HCV-IHC positive cases that did not receive antiviral therapy showed improvement (p=0.015).

Conclusions: Our preliminary results suggest that positive HCV-IHC in post-transplant liver biopsies may identify a subset of patients who may benefit from antiviral therapy who may be difficult to identify on routinely stained biopsy sections (H&E). Additional larger studies (currently in progress) are needed to confirm these findings.

1718 A Broad Immunohistochemistry Panel in Hepatocellular Carcinoma (HCC) Seems to Segregate Molecular Subtypes by Grade: A Cross-Sectional Study in 80 Brazilian Autopsies

A Felipe-Silva, A Wakamatsu, CS Cirqueira, C Cassol, V Alves. University of Sao Paulo, Sao Paulo, SP, Brazil.

Background: Gene expression studies have proposed HCC clustering in different categories. Aggressive types express keratin 19 (CK19), p53 mutation and/or regulation by Met receptor. Less aggressive types retain hepatocyte-like phenotype including molecular subtypes with polysomy of chromosome 7 and activation of beta-catenin.

Design: Eighty autopsies of HCC patients (62 M/18 F, age 58.1 ± 10.9) were studied according clinicopathological data. Immunohistochemistry was performed on tissue microarrays to survey expression of Ki67, cyclin D1, caspase 3, p53, EGFR, Met, CK19, vimentin, beta-catenin, mTOR and kinases ERK1/ERK2. Ki67, cyclin D1 and p53 nuclear staining were analyzed in percentage of labeled cells. CK19 was semiquantified in percentage of positive cells. Nuclear beta-catenin was scored in 0 to 3+. EGFR and other biomarkers were evaluated in a 0–300 score. For correlation analysis we used the Spearman coefficient.

Results: HCV was the major cause (49%), followed by alcoholism (30%) and HBV (19%). Cirrhosis was identified in 90%; advanced tumors in 95%; large vein invasion in 19% and extra-hepatic metastases in 38%. EGFR expression was more frequent in non-tumoral liver (26/26) (P <.05) and in normal controls (8/8) than in primary (60/75) and in metastates (12/17). No control samples showed overexpression of EGFR, which was more common in cirrhotic tissue (17/26) than in advanced tumors (26/72) (P<.05). EGFR overexpression was more frequent in grade 1/2 tumors (P <.01) and in cases with less than four hepatic nodules (P=.01). EGFR expression was correlated to the expression of caspase 3 (P <.01). Expression of ERK1 and ERK2 was correlated to Ki67 and with each other (P<.01), but not to the EGFR expression score. ERK1 was associated with CK19 and vimentin (P<.01) while ERK2 was associated with cyclin D1 (P<.05), Met and membrane beta-catenin (P<.01). CK19, p53 and nuclear beta-catenin were correlated to high grade lesions and to higher rates of cell proliferation (P<.01). Met, EGFR and caspase 3 were correlated with more differentiated lesions. Vimentin was strongly correlated with CK19 (P<.01). mTOR, membrane beta-catenin and cyclin D1 appear to be less associated with histological grade but still associated with cell proliferation by Ki67.

Conclusions: This immunohistochemical approach seems to validate at least two molecular classes of HCC, and histological grade seems to discriminate these groups. We confirmed overexpression of kinases as a key event in tumor progression, but not necessarily associated with overexpression of EGFR.

1719 Radio-Pathologic Correlation and Assessment of Patients with End-Stage Liver Disease and Hepatocellular Carcinoma Undergoing Liver Transplantation

MI Fiel, S Ward, S Thung, A Trivedi, A Fenster, S Florman, TD Schiano. Icahn School of Medicine at Mount Sinai, New York, NY.

Background: Tissue diagnosis for hepatocellular carcinoma (HCC) is not required in the management and listing of patients with HCC undergoing liver transplantation (LT) as the current radiologic imaging modalities are considered adequate and sensitive enough to detect lesions as small as 1 cm. We sought to correlate the radiologic detection with the pathologic assessment of HCC of the explanted specimen as well as evaluate the histological characteristics of the liver.

Design: Patients on the LT waiting list undergo CT scan or MRI every 3-6 months; MRI studies are performed with Eovist. Per protocol, all explanted livers are weighed and sectioned at 0.5cm intervals; sections from all lesions as well as 8 sections of the background liver are processed. Retrospective review was performed by a liver pathologist and assessed for cirrhosis and its severity per the Laennec sub-classification (4A=incomplete cirrhosis, 4B=nodules with thin fibrous septa, 4C=nodules surrounded by thick fibrous septa). Correlation of the number of tumors found on pathological examination with the number of tumors identified by radiological imaging was performed. The time interval between LT and last imaging study was calculated.

Results: Over a 20-month period (1/2012-08/2013), there were 62 adult patients with HCC who underwent LT at our institution. There were 45 M & 17 F, age=59.5+/-7.8 years; 47 had LT for HCV, 5 for steatohepatitis, 4 for HBV, and 6 for other etiologies. Of the total cases, 35/62 (57%, Group A) showed concordance of pathologic and imaging findings whereas 27/62 (43%, Group B) did not. No significant difference in age, sex, time interval between last imaging study and LT, and liver weight was seen between Group A and Group B. 33 of 35 in Group A and 26 of 27 in Group B had cirrhosis. Fewer group A (17/33) than group B (22/26) patients had cirrhosis class 4C (p=0.008). Among Group B cases, 18/27 (67%) had tumors >/= 1cm that were not detected by pre-LT imaging.

Conclusions: In our cohort, a high rate of discrepancy was identified between pathological assessment as compared to HCC identified on imaging studies. This may be explained by the more advanced cirrhosis in those patients whose HCC were not identified on imaging studies. Even at a large transplant center with frequent protocol imaging studies and an experienced team of radiologists, some HCC lesions may still be difficult to identify by radiology.

1720 Relationship of B-Catenin Activation and Myc in Hepatocellular Adenoma and Hepatocellular Carcinoma

G Genrich, N Joseph, K Evason, S Kakar. UCSF, San Francisco, CA.

Background: β-catenin activation occurs in a subset of hepatocellular adenomas (HCA) and hepatocellular carcinomas (HCC). Diffuse staining for glutamine synthetase (GS) is considered a marker of β-catenin activation, but there is limited data on the expression and significance of other β-catenin target genes such as *MYC* in HCA and HCC.

Design: Immunohistochemistry for β-catenin, GS and Myc was performed in cases of HCA (n=25) and HCC (n=83). Cases with nuclear β-catenin, and/or diffuse strong GS staining were considered β-catenin activated. The correlation of Myc staining with β-catenin activation and clinicpathologic features was examined.

Results: β-catenin activation and Myc positivity were seen in 30 (36%) and 24 (29%) of HCCs respectively. Myc staining was positively correlated with nuclear β-catenin staining (p=0.001, see Table) and β-catenin activation (p=0.007) in HCC. HCCs with positive Myc staining and β-catenin activation were more likely to be poorly differentiated (50%) than tumors without positive staining for these markers (21%) (P=0.024). β-catenin activation and Myc positivity were seen in 3 (12%) and 7 (28%) of HCAs, respectively. There was no correlation of Myc expression with clinicopathologic features and β-catenin activation in HCAs.

Correlation of Myc staining and β-catenin staining in HCC

	Myc positive staining	Myc negative staining
β-catenin positive staining	13 (62%)	8 (38%)
β-catenin negative staining	11 (18%)	51 (82%)
β-catenin activated	14 (47%)	16 (53%)
β-catenin inactive	10 (19%)	43 (81%)

Conclusions: β-catenin activation is positively correlated with Myc staining in HCC, supporting the hypothesis that Myc may be a target gene for β-catenin in HCC. β-catenin activated HCC tend to be well differentiated; however, this series shows that HCC with combined Myc expression and β-catenin activation tend to be poorly differentiated, suggesting that Myc expression may play a role in acquisition of an aggressive phenotype in β-catenin activated HCC.

1721 Evaluation of a Proposed Set of Histologic Features to Distinguish Drug-Induced Liver Injury and Autoimmune Hepatitis

P Gopal, S Hammer, L Peng, Y Fang, AG Singal. University of Texas Southwestern Medical Center, Dallas, TX.

Background: Histologic distinction between autoimmune hepatitis (AIH) and drug-induced liver injury (DILI) on liver biopsies is an ongoing diagnostic challenge for pathologists. Accurately differentiating the two entities is critical given both entities can result in severe liver injury and proper management is imperative for positive patient outcomes. Suzuki and colleagues recently developed a model to histologically discriminate AIH and DILI without the need for clinical information. The aim of our study is to externally validate the proposed model in a cohort of patients with AIH and DILI.

Design: We evaluated liver biopsies from clinically well-characterized cases of AIH and DILI, with all diagnoses independently confirmed through chart review by an experienced hepatologist. Biopsy slides were independently evaluated by two liver-fellowship trained pathologists, who were blinded to clinical information. Histologic data was collected for each case using standardized forms, including but not limited to presence of portal inflammation, intra-acinar lymphocytes, intra-acinar eosinophils, canilicular cholestasis, portal plasma infiltrates, rosette formation, and fibrosis. We determined the inter-observer agreement rate and concordance rate between clinical diagnosis and histologic diagnosis.

Results: We included 19 cases (10 AIH, 9 DILI). One pathologist correctly identified 84.2% of cases and the other pathologist correctly identified 66.7% of cases. The concordance rate for diagnosis was low at 46.7% between the pathologists– 57.1% among AIH cases and 37.5% among DILI cases. For specific histologic features, concordance was high at 89.5% for presence of portal inflammation, intermediate at 68.4% for presence of intra-acinar lymphoctes, intra-acinar eosinophils, and portal tract plasma cells but low at 47.4% for rosette formation. The proposed scoring system decreased the proportion correctly classified to 63.2% for the first pathologist but increased the proportion to 73.7% for the second pathologist. The scoring system correctly classified all four cases labeled as indeterminate by the pathologists.

Conclusions: Although there are potential histologic differences between AIH and DILI, many cases have overlapping features that can preclude accurate diagnosis using histology alone. Scoring systems to distinguish the two entities may be helpful in indeterminate cases but appear to be limited by operator dependency and low inter-observer agreement.

1722 Pathologic Correlation of Nodules and Transarterial Chemotherapy Embolization (TACE) Effect in Livers with Hepatocellular Carcinoma

B Goyal, KJ Fowler, N Saad, EM Brunt. Washington University School of Medicine, St. Louis, MO; Mallinckrodt Institute of Radiology, St. Louis, MO.

Background: Hepatocellular carcinoma (HCC) is an aggressive tumor which usually arises in cirrhosis. Patients may undergo TACE to bridge to orthotopic liver transplantation (OLT). We aim to investigate the effectiveness of TACE and the radiology-pathology (R-P) correlation in explant hepatectomies.

Design: 46 consecutive patients (1/1/11-12/30/12) with clinically diagnosed HCC who underwent TACE prior to OLT had post-TACE radiology and explant pathology available for review. Standard grossing practice at our institution includes submission of entire TACEd nodules based on post-TACE radiology as well as one section of any suspicious nodule. TACE effectiveness was defined as a percentage of nodule necrosis.

Results: 82 nodules identified by R and P had agreement for location. Of these, 71 nodules (86%) had R and P diagnostic agreement. Nodules in diagnostic disagreement were, by P, multifocal HCCs(3), other primary liver cancers (2), HCCs in dysplastic nodules (2), HCCs (2), and benign lesions (2). 66 nodules were identified by P-only; 19 nodules were identified by R-only. Table 1 summarizes nodules identified by R-only or P-only.

	R	P
HCC	2	46
Indeterminate	11	-
Dysplastic Nodule	4	7
Macroregenerative Nodule	-	10
Other	1	3

Of the P-only nodules, 20 ranged from 1.0-3.0 cm and were diagnosed by P as multifocal HCCs(7), HCCs (7), dysplastic nodules (2), and macroregenerative nodules (4). The remaining 26 P-only nodules measured <1.0 cm. The R-only nodules ranged from 0.6-2.5cm. 60 nodules with R-P agreement in location and diagnoses underwent TACE. Figure 1 summarizes the effectiveness by both R and P. Agreement was considered if effectiveness was +/- 10% by both R and P. 32 TACEd nodules (53%) were in R-P agreement as to effectiveness of treatment.

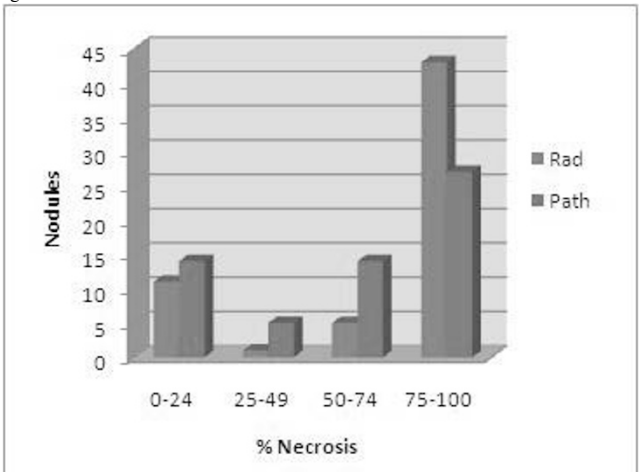

Conclusions: R-P discrepancies most often occur with multifocal HCCs and other primary liver cancers. Discrepancies may be attributed to altered anatomy in the setting of cirrhosis. There is an overestimation of the effectiveness of TACE by radiology and limited correlation in R-P estimates of TACE effectiveness.

1723 Comparison of Novel Albumin In Situ Hybridization RNAScope Method to Other Markers of Hepatocellular Phenotype

RP Graham, JA Vrana, ME Law, KL Grogg, T-T Wu, T Mounajjed. Mayo Clinic, Rochester, MN.

Background: Detection of albumin mRNA in formalin fixed paraffin embedded tissue has been used to support hepatocellular phenotype in carcinomas. A novel in situ hybridization (ISH) RNAScope method was developed to detect albumin mRNA transcripts with higher sensitivity and less background than prior RNA ISH assays. We compared albumin expression by ISH RNAScope to established markers of hepatocellular phenotype.

Design: Resection or large biopsy specimens from 27 hepatocellular carcinomas (HCC) (including 5 HCCs metastatic to bone), 35 intrahepatic cholangiocarcinomas (ICC), and 23 neuroendocrine carcinomas (NECA) metastatic to the liver were selected. Hematoxylin and eosin stained sections were reviewed and appropriate blocks selected for immunohistochemistry (IHC) and ISH. The final diagnosis for each case was confirmed by examining clinical and radiologic records. IHC for Arginase 1, HepPar 1, Glypican 3 and polyclonal CEA (pCEA) was performed using commercially available antibodies and established methods. For all markers, distinct staining in≥5% of tumor cells was considered positive. Canalicular pCEA expression was supportive of HCC. Albumin ISH (Advanced Cell Diagnostics, CA) was performed using the manufacturer's enclosed method. Expression of all markers was also evaluated in the background liver.

Results: Albumin ISH was positive in 96% of HCC, 40% of ICC and 22% of NECAs. Albumin ISH positive-ICCs included 9 of 15 (60%) well-differentiated, 7 of 17 (41%) moderately differentiated and 0 of 3 poorly differentiated tumors. Albumin ISH was characterized by strong diffuse staining in all positive cases. Albumin ISH was also positive in normal bile ducts. Arginase 1 was positive in 93% of HCC, 0% of ICCs, and 1 NECA. Both HCCs negative for Arginase 1 were decalcified and the single positive NECA showed weak staining. The sensitivity of albumin ISH and Arginase 1 for the diagnosis of HCC was 96% and 93% and their specificity was 70% and 99%, respectively. HepPar1, pCEA and Glypican 3 were positive in 89%. 81% and 78% of HCC, and 0%, 13% and 39% NECAs, respectively.

Conclusions: The new ISH method for detection of albumin mRNA displays excellent sensitivity for HCC but is hampered by low specificity, predominantly due to positivity in ICCs. This may result from low levels of albumin mRNA expression in bile ducts and ICCs. This hypothesis requires further study. Arginase 1 appears to be a superior marker for HCC compared to ISH. Arginase 1 showed sensitivity comparable to ISH for HCC and was more specific. Arginase 1 but may be of limited utility in decalcified sections.

1724 Concurrent Activation of Acetylation and Tri-Methylation in H3K27 Occurs in a Subset of Hepatocellular Carcinoma with Aggressive Behavior

A Hayashi, N Yamauchi, J Shibahara, H Kimura, T Morikawa, S Ishikawa, G Nagae, N Kokudo, H Aburatani, M Fukayama. Graduate School of Medicine, The University of Tokyo, Bunkyo-ku, Tokyo, Japan; Graduate School of Frontier Biosciences, Osaka University, Suita, Osaka, Japan; Medical Research Institute, Tokyo Medical and Dental University, Bunkyo-ku, Tokyo, Japan; Research Center for Advanced Science and Technology, The University of Tokyo, Meguro-ku, Tokyo, Japan.

Background: Hepatocellular carcinoma (HCC) is one of the major cancers worldwide. Accumulating evidence has shown that not only genetic, but also epigenetic changes play crucial roles in the genesis and prognosis of cancer. The global levels of several histone modifications and their modification enzymes have clinical significance in several cancers. In the present study, we focused on the acetylation and tri-methylation of lysine 27 on histone H3 (H3K27ac and H3K27me3, respectively), since these modifications are known to act in opposite directions.

Design: Neoplastic and non-neoplastic tissues from 198 HCC cases were immunostained with specific monoclonal antibodies against H3K27ac and H3K27me3. The stained tissues were evaluated by an image analysis program with output of histological scores (H-scores), obtained by multiplying the percentage of positive cells (0–100%) by the classified IHC marker intensity (0–3) (range: 0–300).

Results: The HCC tissues showed significantly higher H-scores for H3K27ac (156.7±86.8) and H3K27me3 (151.8±78.1) than the background livers (40.3±33.0 and 64.7±45.6, respectively) (both P<0.001). Concurrently activated cases, high-H3K27ac/high-H3K27me3 scores (n=54), showed significant correlations with poorly differentiated morphology (P<0.01) and p53-positive staining (P<0.05), and poor prognosis (P<0.01). By confocal microscopy, H3K27ac was present in central euchromatin regions, while H3K27me3 was detected in peripheral heterochromatin regions, of individual cancer cells.

Conclusions: Concurrent activation of acetylation and methylation at H3K27 occurs in HCC cells in association with p53 abnormalities, although the two modifications occupy different regions of the nuclei.

1725 Liver Fibrosis Evaluated by the Ishak Method Identifies Differences in Cancer Survival of Hepatitis B Patients with Early vs. Advanced Cirrhosis

SP Hiotis, HS Kadri, S Blank, Q Wang, W Luan, PA Deaderick, A Zhu, MI Fiel. Icahn School of Medicine at Mount Sinai, NY, NY.

Background: The Scheuer system of staging HBV fibrosis is most often used by pathologists, but the modified Ishak method distinguishes early or incomplete cirrhosis (stage 5) from established cirrhosis (stage 6). Studies have found worse cancer outcomes in HBV-associated hepatocellular carcinoma (HCC) patients with Ishak 6 vs. 1-5; hence, it is important to differentiate them for research. We compared data from re-reviews of pathology specimens to data from pathology reports, determined the distribution of Ishak stages among cases and assessed for differences in survival following hepatectomy in HBV-HCC patients according to Ishak and Scheuer stage.

Design: Re-reviews of specimens from HBV-HCC patients treated by hepatectomy at a Western institution from 1988-2013 were performed by a liver pathologist blinded to patient data. Non-neoplastic liver tissue was evaluated for Ishak stage (0-6) and Scheuer stage (0-4). Scheuer stages assigned at the time of resection were obtained from electronic pathology reports. Agreement between Scheuer stage from re-review and pathology reports was assessed by a weighted kappa statistic. Contingency tables were used to compare Scheuer and Ishak stage according to re-review, and Kaplan-Meier analysis evaluated 5-year survival rates of patients by Ishak and Scheuer fibrosis stage.

Results: Re-reviews of 285 HBV-HCC cases were available. There is substantial agreement between Scheuer stage from reviewed data vs. pathology reports (weighted Kappa = 0.64 (p<0.001), 95% CI 0.57-0.71). According to re-reviews, 99% of patients with Scheuer 4 had Ishak 5-6; of these 133 patients, 59% had Ishak 6. Kaplan-Meier curves of Scheuer and Ishak stages showed similar survival rates; however, curves of Ishak 5 and 6 appeared separated.

Figure 1. Five-year survival of HBV-HCC patients according to Ishak fibrosis stage and Scheuer fibrosis stage.

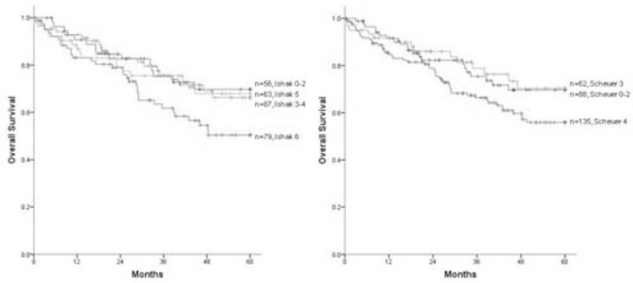

Conclusions: Pathologist re-review of liver specimens is the most accurate way to evaluate fibrosis. Agreement between re-review and clinical report is high, but enough disparity exists to emphasize the need for reviews of pathology specimens for research. The Ishak method is advantageous over the Scheuer system because it distinguishes early or incomplete cirrhosis (Ishak 5) from cirrhosis (Ishak 6), which exhibit different cancer outcomes that are not observed if using the Scheuer system.

1726 Metastases of Hepatocellular Carcinoma to Vertebrae: A 'Significant Other' Preferred Route of Distant Metastases

R Jain, I Lamzabi, S Jakate, P Gattuso. Rush University Medical Center, Chicago, IL.

Background: Distant metastases from hepatocellular carcinoma (HCC) are rare. When these occur, the most common route of metastasis is understood to be invasion into portal and hepatic vein radicles and extension into inferior vena cava (IVC) leading to lung metastases. Regional metastases to lymph nodes are also known to occur. We observed that many of our patients presented with vertebral metastases and therefore hypothesized that there might be an alternate route of possible spread which has not been well explored before. The branches of portal veins freely anastomose through lumbar veins with vertebral venous plexus across the bare area of liver. Both of these venous systems are valveless. We undertook this study to investigate the whether this anastomosis could be a significant contributor to the spread of the tumor.

Design: We searched our Medical Center's (University Hospital with orthotopic liver transplant program) database for patients with HCC with metastasis between Nov 1992 and Aug 2013. Clinical, radiological and pathological features were reviewed. The diagnosis of metastases was established by characteristic radiographic appearance and/or histological confirmation.

Results: There were a total of 287 patients diagnosed with HCC during this period. 22 (8%) patients (15 males and 7 females) presented with metastases. 15 patients (69%) had bone metastases, 13 (87%) of whom had lesions in the vertebral column (preferentially lumbar and thoracic). Only 1 patient had extension of tumor into the IVC. Only this patient had metastases to both lungs and spine. 7 (32%) patients had non-osseous metastasis and 6/7 had lung metastasis. Irrespective of the site of metastasis, the most common primary liver disease was cirrhosis and HCV hepatitis. In 7 patients, the metastases presented after orthotopic liver transplantation although the graft was unaffected in all.

Conclusions: Metastases in HCC are uncommon, but when they occur, lumbar and thoracic vertebrae appear to be preferred target site. Anastomoses between vertebral and portal venous plexuses across the bare area of the liver may potentially provide this significant alternate route of access. From our data, it also appears that vertebral and lung metastases are often mutually exclusive, hence the caval and vertebral routes of tumor spread appear to be independent of each other. We propose that apart from lungs, special attention should be paid to detection of metastasis in the vertebral column.

1727 Ipilimumab Induced Hepatitis: Clinicopathologic Characterization in a Series of Seven Cases

M Johncilla, J Misdraji, A Srivastava, DS Pratt, LA Doyle. Brigham and Women's Hospital and Harvard Medical School, Boston, MA; Massachusetts General Hospital, Boston, MA.

Background: Ipilimumab is a monoclonal antibody used in the treatment of metastatic melanoma that inhibits CTLA4, a receptor on cytotoxic T lymphocytes, resulting in cytotoxic tumor cell death. Liver toxicity is rare. The aim of this study was to characterize the histologic features of ipilimumab induced hepatitis.

Design: 7 patients with abnormal liver function tests (LFTs) and clinical suspicion of ipilimumab induced hepatitis who underwent liver biopsy were identified over a 5 year period. Histologic, immunophenotypic and clinical features were evaluated.

Results: All patients were male (median age 63 years, range 33 – 83) and presented with abnormal LFTs after 1-4 doses of ipilimumab. None had pre-existing liver disease. Viral (HBV, HCV) serologies, ANA, and AMA were negative in all. 4/7 biopsies showed features resembling autoimmune hepatitis (AIH), 2/7 showed steatohepatitis and 1/7 showed predominantly portal hepatitis. Biopsies from patients with AIH-like pattern showed moderate-severe lobular, portal and periportal inflammation composed predominantly of CD8+ T lymphocytes, scattered plasma cells and eosinophils. Prominent histiocytic sinusoidal infiltrates were present in 3 cases. 1 case had mild cholestasis. Patients with AIH-like pattern had elevated ALT (range 377–3075U/L), AST (143–1293U/L) and total bilirubin (TB) (0.4–15.6mg/dL), and modest elevations in alkaline phosphatase (AP) (302–453U/L). 1 patient was obese. Patients with steatohepatitis had modest transaminitis: ALT (156–575U/L), AST (220–377U/L), and normal TB and AP; both had risk factors for fatty liver (1 obesity, 1 alcohol). 1 patient had neutrophil rich, predominantly portal, inflammation and had elevated AST, ALT, and AP, and normal TB. Mild bile duct injury was seen in 2 cases (1 AIH-like & 1 steatohepatitis pattern). Central endothelialitis and perivenular collapse was present in 6/7 cases. None had fibrosis. Discontinuation of ipilimumab and administration of immunosuppressives resulted in improved LFTs in all patients within 2-3 months of presentation.

Conclusions: Ipilimumab-induced hepatitis most commonly presents with an AIH-like pattern. Central vein damage with endothelialitis & perivenular collapse, and prominent sinusoidal histiocytic infiltrates are also commonly seen. Steatotic and portal predominant patterns of injury are uncommon and can only be recognized with certainty after cessation of the drug leads to normalization of LFTs. Steatohepatitis secondary to ipilimumab may represent exacerbation of pre-existing fatty liver disease.

1728 Clinical and Pathologic Analysis of Liver Biopsies in Patients with Fontan Circulation

M Johncilla, FM Wu, C Ukomadu, K Gauvreau, R Odze. Brigham and Women's Hospital, Boston, MA; Boston Children's Hospital, Boston, MA.

Background: The Fontan procedure is used to treat patients with a single functional heart ventricle. It involves direct connection of the superior and inferior vena cava to the pulmonary circulation ('Fontan circulation'). These patients sometimes present with hepatic dysfunction thought to be due to chronically raised systemic venous pressures. The aim of this study was to evaluate the pathologic features of a large cohort of patients with Fontan circulation and to correlate the findings with a wide variety of clinical and lab data related to the health of the patient and liver function.

Design: 67 adults with Fontan circulation were enrolled from 6 US adult congenital heart centers. For each individual, demographics, clinical history, a liver biopsy and numerous imaging and serological data, including time from Fontan procedure to biopsy and hepatic vein pressure gradient, were obtained as clinically indicated. Liver biopsies were reviewed for the presence and degree of sinusoidal fibrosis, sinusoidal dilatation, steatosis, inflammation and portal/septal fibrosis using a 6 tier METAVIR fibrosis scale.

Results: There were 32 males and 35 females of (mean 32 yrs). All 67 cases (100%) showed sinusoidal dilation, 43 of which showed dilation in greater than 1/3 of sinusoids. 60 (90%) cases showed varying degrees of sinusoidal fibrosis, 40 of which showed fibrosis in greater than 1/3 of sinusoids. 60 cases (90%) showed portal/septal fibrosis with 18 cases showing bridging fibrosis, 18 showing evolving cirrhosis and 4, established cirrhosis. Modified METAVIR fibrosis scores correlated positively with hepatic vein pressure gradient, albumin and Hgb A1C levels. Sinusoidal dilation correlated with type of initial Fontan, positive correlations included AlkPhos and negative correlations included hematocrit and albumin ($p<0.05$ for all). There was no correlation with Fibrosure scores, hyaluronic acid, INR, time to biopsy or any composite scoring systems used to monitor liver and overall health, with any of the histologic parameters. Inflammation and steatosis were minimal to absent in all cases.

Conclusions: Fontan circulation induced liver injury often results in sinusoidal dilation and significant fibrosis or cirrhosis. Extent of sinusoidal dilation and METAVIR fibrosis score correlates with multiple clinical parameters used to assess liver health including hepatic vein pressure gradient. Thus, histopathology of the liver remains the most useful diagnostic test and liver-health measure in these patients.

1729 Digital Image Analysis Shows Variation in Glutamine Synthetase Staining of Focal Nodular Hyperplasia

C Kavran, MM Yearsley, X Zhou, BJ Swanson. The Ohio State University Wexner Medical Center, Columbus, OH.

Background: Focal nodular hyperplasia (FNH) is a benign lesion that can be difficult to distinguish from hepatocellular adenoma (HCA). Glutamine synthetase (GS) staining can differentiate these two entities by its pattern of staining, which is map-like in FNH, but perivenular in HCA. While GS is often helpful, we have observed variant staining of GS in FNH. This can lead to diagnostic difficulties, especially in biopsy specimens. To better understand this variation, we objectively measured GS staining of FNH in resection specimens by digital image analysis.

Design: Thirty FNHs with classic histologic features were selected from archives and stained with GS. One representative slide from each case was examined. Digital slide images were produced with the Aperio ScanScope XT (Vista, CA). Tissue Studio 3.5 software by Definiens (Munich, Germany) was used to analyze component pixels, leading to quantification of the intensity of GS in hepatocytes only. Fibrous bands were excluded from analysis. The percentage of hepatocytes within the lesion with high intensity GS staining was calculated. This was correlated with lesion size, age and sex.

Results:

GS staining and clinicopathological variables in FNH

	Low GS Staining	Usual GS Staining
Average Size (cm)	1.5 +/- 1.4	4.3 +/- 3.3
Average Age (yr)	39.5 +/- 21.9	36.3 +/- 12.5
Sex	50% Male	15% Male

Twenty-six cases had the usual map-like GS staining pattern with an average GS staining of 34% (range 19-54%). Four FNHs had low GS staining (range 2-13%) that was still map-like in most cases (n=3). These 4 cases had classic H&E features and no adjacent mass lesion. There was a trend between the size of FNH and low GS staining ($p=0.11$). There was no significant association between low GS staining and patient age or sex.

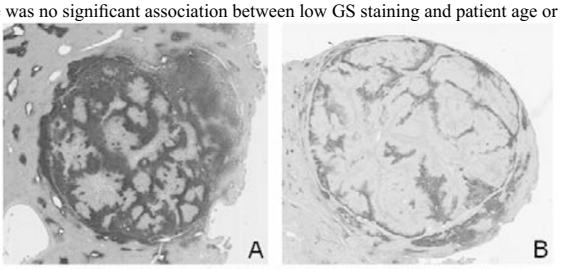

FNH with usual GS staining (A) and aberrantly low GS staining (B).

Conclusions: While most FNHs had the expected map-like positivity with GS, a small subset (14%) showed low GS staining. GS staining did not correlate with lesion size, patient's age or sex. This aberrant staining could potentially be a diagnostic pitfall in the distinction of FNH from HCA, especially in biopsy samples with limited tissue present. Thus, H&E criteria should be utilized in conjuction with GS staining in the evaluation of liver lesions.

1730 The Histologic Spectrum of Hematopoietic Neoplasms Involving the Liver: A Single Institution Review

SM Kirby, G Lozanski, BJ Swanson. The Ohio State University Wexner Medical Center, Columbus, OH.

Background: Hematopoietic neoplasms involving the liver, although infrequently biopsied, may cause diagnostic pitfalls. Reasons for biopsy include diagnosis of a mass lesion or sampling in a patient with clinical or laboratory signs of liver disease. These neoplasms may be difficult to distinguish from medical liver diseases and may have different biological behaviors compared to their non-hepatic counterparts.

Design: A computerized laboratory database search revealed 99 hematopoietic neoplasms from 98 patients with a liver needle biopsy (n=89) or excision specimen (n=10), with an age range of 28 to 87 years old. Slides and available clinical histories were reviewed.

Results: Key results are summarized in Table 1. Overall, 77% of cases had a history of lymphoma, while 23% represented new diagnoses. On radiology, 55% of cases had lymphadenopathy, 76% presented with a mass, while 24% had either diffuse changes or no radiologic abnormality. Microscopically, 73% of cases displayed a primarily diffuse pattern, while 22% were portal and 4% were sinusoidal. Additionally, among diffuse large B cell lymphomas (DLBCL), 74% of cases showed high proliferation index (>70%). 73% of DLBCLs with sufficient material for classification were of GC type.

Table 1. Summary of cases

Diagnosis	Percent of Total	Initial Diagnosis in Liver	Liver-restricted	Radiologic Mass Lesion	Primary Microscopic Pattern	HIV Positivity	Hep C Positivity
DLBCL (n=38)	39%	32%	5%	92%	diffuse (95%)	17%	30%
Classical Hodgkin lymphoma (n=16)	16%	94%	0	86%	diffuse (93%)	7%	14%
Chronic lymphocytic leukemia/small lymphocytic lymphoma (n=15)	15%	87%	0	42%	portal (79%)	0	29
Plasma cell neoplasm (n=7)	7%	0	0	67%	diffuse (83%)	0	0
Post-transplant lymphoproliferative disorder (n=7)	7%	0	0	100%	diffuse (100%)	20%	40%
Marginal zone lymphoma (n=4)	4%	50%	50%	75%	diffuse (75%)	0	33%
T cell lymphoma (n=4)	4%	0	0	25%	portal (50%)	0	0
Acute myeloid leukemia (n=2)	2%	0	0	50%	diffuse (50%), portal (50%)	0	0
Burkitt lymphoma (n=2)	2%	0	0	100%	portal (100%)	50%	50%
Mantle cell lymphoma (n=1)	1%	0	0	100%	portal (100%)	NA	NA
Langerhan cell histiocytosis (n=1)	1%	0	0	0	portal (100%)	0	0

Conclusions: Most cases in this cohort presented as mass lesions in patients with systemic disease. However, low grade lymphomas often presented with minimal radiologic findings and subtle histologic findings, such as mild portal infiltration, resembling chronic hepatitis. This data suggests that hepatic DLBCL may differ

immunohistochemically and biologically from systemic DLBCL, with higher proliferation indices and a higher percentage of germinal center phenotype and thus warrants further studies.

1731 Fibrosis Progression in Adult Non-Alcoholic Fatty Liver Disease: Association with Severity of Histological Features

DE Kleiner, EM Brunt, L Wilson, PH Belt, CD Guy, MM Yeh, KV Kowdley, AJ Sanyal, BA Neuschwander-Tetri. National Cancer Institute, Bethesda, MD; Washington University, St. Louis, MO; Johns Hopkins Bloomberg School of Public Health, Baltimore, MD; Duke University, Durham, NC; University of Washington, Seattle, WA; Virginia Mason Medical Center, Seattle, WA; Virginia Commonwealth University, Richmond, VA; Saint Louis University, St. Louis, MO.

Background: Non-alcoholic fatty liver disease (NAFLD) has a complex natural history with only a fraction of patients progressing to cirrhosis and its complications. Using paired biopsies one is able to detect gradual changes in fibrosis and other features long before a patient develops clinical cirrhosis. The aim of this study was to examine the association of the severity of individual histological features and progression when the score of particular features remained unchanged from the first biopsy to the last.

Design: Adult patients enrolled in one of the NASH CRN studies with 2 or more biopsies (excluding active treatment arms of the PIVENS study) at least a year apart were included. All biopsies underwent blinded consensus review using the NASH CRN system. Pairs of biopsies in which scores for particular features were unchanged were analyzed for fibrosis progression that was related to the severity of that feature using the Cochran-Armitage Trend test.

Results: 359 patients (mean age 47 years, 64% female) had at least 2 biopsies, with a mean time between biopsies of 4.4 years (range 1 to 17.3). For some histological features, when the semi-quantitative score remained unchanged from first to last biopsy, the severity of that feature was associated with fibrosis progression (TABLE). The severity of steatosis and lobular inflammation was not associated with fibrosis progression in this model.

Unchanged Histological Finding	N	p value
Ballooning	166	0.007
Mallory Bodies	270	0.003
Acidophils	230	0.003
Portal Inflammation	214	0.02
NAFLD Activity Score (NAS)	64	0.046
NAS <= 1 point change	190	0.004

Conclusions: When particular histological features remain unchanged over time, the relative severity of those features at baseline is associated with the risk of fibrosis progression. Therapies that improve these histological features may have more impact on overall disease progression.

1732 Histologic Comparison of Non-Tumor Liver in Hepatocellular Carcinoma Patients Treated with Yttrium-90 Radioembolization and Transcatheter Arterial Chemoembolization

HM Ko, SC Ward, M Facciuto, E Kim, RS Patel, D Robinson, AM Fischman, TD Schiano, MI Fiel. Icahn School of Medicine at Mount Sinai, New York, NY.

Background: Intra-arterial radio-embolization using Yttrium-90 (Y90) microspheres and transcatheter arterial chemoembolization (TACE) are both effective therapeutic techniques in hepatocellular carcinoma (HCC). Both can induce atrophy and fibrosis of the adjacent liver. Recently, high-dose Y90 has been used to treat HCC. The histological features associated with this treatment in the non-tumoral liver have not been fully elucidated. We compared the histological features of patients with HCC treated with high-dose Y90 and TACE.

Design: We identified 4 patients with HCC who received high-dose Y90 and then underwent resection (n=2) or liver transplantation (LT) (n=2), and 4 HCC patients treated with TACE who then underwent LT. Retrospective review of slides were assessed by 3 pathologists in three regions (peritumoral <1cm from HCC, ipsilateral lobe >1cm from HCC, and contralateral lobe) for: degree of sinusoidal obstructive syndrome (SOS), parenchymal collapse, fibrointimal vessel wall thickening, and cytological changes in bile ducts, ductules and endothelial cells. Clinical data regarding the liver volume, dosage of radiation, original tumor size and time between treatment and surgery were collected. Data were analyzed by T-test and chi square.

Results: The Y90 dose ranged from 100-150G. The Y90 changes were most apparent in the peritumoral liver. Diffuse SOS was seen in the peri-tumoral areas in 3 of 4 Y90 cases and in none of the 4 TACE cases ($p<0.05$). Fibrointimal thickening and cytological changes in the bile duct/ductules and endothelial cells were seen in the peri-tumoral liver in all 4 Y90 cases whereas none were seen in TACE cases. Parenchymal collapse was significantly higher in the Y90 treated tumors compared to TACE (77.5%, 15%, $p< 0.005$).

Conclusions: Intra-arterial Y90 therapy is a useful modality for treatment of patients with HCC and is also associated with changes in the ipsilateral lobe. In particular, SOS appears prominent in the peritumoral liver. SOS is likely due to endothelial damage similar to veno-occlusive disease seen after ablative radiation, and may also explain the significant atrophy and fibrosis of the ipsilateral lobe.

1733 Small Cell Clusters with High Expression of miR-21 in Human Hepatocellular Carcinoma Show Intermediate Phenotype as Well as a Close Association with Fibrous Stromal Reaction

A Kumagai, Y Takahashi, S Morita, T Aso, H Uozaki, T Fukusato. Teikyo University School of Medicine, Tokyo, Japan.

Background: Expression of microRNA-21 (miR-21) is reported to be increased in many cancers including hepatocellular carcinoma (HCC). However, the role of increased expression of miR-21 in HCC remains to be clarified. We performed in situ hybridization analysis for miR-21 in HCC tissues to characterize cellular phenotype and localization of miR-21-positive tumor cells.

Design: Formalin-fixed paraffin-embedded tissue samples from 48 patients with HCC (43 men and 5 women; age range, 44-82 years) were examined. In situ hybridization analysis using locked nuclear acid probe was performed to determine the expression of miR-21. Tumor tissues were also immunostained for HepPar1, CK7, CK19, EpCAM, NCAM, c-kit and CD133. The relationship between miR-21 expression and clinicopathological parameters of HCC including hepatitis virus status, differentiation grade, tumor size, the amount of fibrous stroma, and existence of liver cirrhosis was also evaluated.

Results: miR-21-positive tumor cells were shown in 27 (56.2 %) of 48 HCC cases but there was no correlation between miR-21 positivity and clinicpathological parameters in HCCs. Sixteen of 27 miR-21-positive HCCs contained small tumor cell clusters with intense positivity for miR-21. The small cell clusters with high expression of miR-21 were composed of trabecular tumor cell nests with small oval or round nuclei, unclear nucleolus, scanty cytoplasm, and high nuclear/cytoplamic ratio and were more frequently found in HCCs with dense fibrous stroma than without it ($p<0.001$). In addition, the small cell clusters of HCC were positive for CK7 immunostaining but negative for HepPar-1, and demonstrated immunoreactivity to hepatic progenitor cell markers such as CK19, EpCAM and NCAM.

Conclusions: Small HCC cell clusters with high expression of miR-21 showed morphological and immunohistochemical phenotypes of intermediate cells, suggesting hepatic progenitor cell origin, as well as a close association with fibrous stromal reaction in HCC.

1734 Can Hypoxia after Transarterial Chemoembolization (TACE) Trigger a Progenitor/Cholangiocytic Cell Phenotype in Hepatocellular Carcinoma?

J-P Lai, BS Knudsen, M Guindi. Cedars-Sinai Medical Center, Los Angeles, CA.

Background: TACE causes anoxia in hepatocellular carcinoma (HCC), with necrosis of HCC cells. In some cases residual/recurrent (r/r) HCC is present on explant pathology. Hypoxia has been associated with aggressive cancer biology. We hypothesized that CK19, a cholangiocytic/progenitor marker, and (hepatocyte growth factor/scatter factor) HGF, a pro-metastatic cytokine, maybe expressed in hypoxic r/r HCC after TACE.

Design: From 2008 - 2013, we identified 68 liver explants with previous TACE, of these 15 had r/r HCC. 9 out of these 15 cases had other untreated HCC nodules away from TACE, used as controls. Imunohistochemistry included CAIX, CK19, EpCAM (Ber-EP4) and Hepar1 and double staining for CAIX and CK19. Immunohistochemical profiles were generated by 3 pathologists.

Results: Expression of CAIX was positive in 8/15r/r HCCs (53%) in areas adjacent to TACE-induced necrosis. CAIX expression was not observed in untreated HCCs except for one case (11%). CK19 and EpCAM were coexpressed with CAIX in 3 of 8 cases (38%), but not in CAIX negative tumors. Double staining of CAIX and CK19 showed co-localization in 40-50% of tumor cells. Hepar1 was negative in one CAIX/CK19 positive area of morphologically conventional r/r HCC. HGF expression was increased in 2 of 3 CAIX positive areas. Surprisingly in bile ducts and ductules, not compromised by hypoxia, CAIX was expressed in a large subpopulation of CK19 positive cholangiocytes.

Conclusions: Hypoxia may trigger the expression of proteins normally associated with cholangiocytic/progenitor cell differentiation, suggesting that TACE paradoxically causes an aggressive tumor phenotype. In addition, CAIX expression occurs in bile ducts and ductules independent of hypoxia.

1735 Tumoral Heterogeneity of Intrahepatic Cholangiocarcinomas Revealed by MALDI Imaging Mass Spectrometry

J Le Faouder, S Laouirem, T Alexandrov, S Ben-Harzallah, M Albuquerque, P Bedossa, V Paradis. INSERM U773, Clichy, France; Center for Industrial Mathematics, Bremen, Germany; Beaujon Hospital, Clichy, France.

Background: Cholangiocarcinoma (CC), the second most common primary malignancy of the liver arising from biliary epithelial cells, is characterized by a desmoplastic stroma. Two main subtypes of intra-hepatic CC, hilar (H) and peripheral (P), are described according to their localization. The objective of the study was to compare, using MALDI imaging mass spectrometry (MALDI IMS), proteomic profiles of H and P-CC, in order to assess specific differential markers between both subtypes and describe their respective localization within tumor samples.

Design: Twenty-seven CC (16 P-CC and 11 H-CC) were subjected to MALDI IMS. Proteomic data were submitted to a dedicated cross-classification comparative design, allowing the comparison of the whole generated spectra. Immunohistochemistry was performed for validation.

Results: Comparative analysis yielded a list of 19 differential protein peaks between both subtypes, 14 of them overexpressed in H-CC. Of these, human neutrophil peptides 1-3 were overexpressed mainly by tumor cells as well as inflammatory and endothelial cells, whereas S100 proteins (A6 and A11) were restricted to stromal area. By contrast, Thymosin β4, overexpressed in P-CC, was distributed in carcinomatous and stromal parts.

Conclusions: These results highlight the potential of MALDI IMS to uncover new relevant biomarkers of CC and support heterogeneity of the 2 different subtypes and their intratumoral heterogeneity as well.

1736 Clinical and Histologic Characterization of Steatotic HCV Liver Biopsy: Central Portalization Correlates with Fibrosis but Not with Risk Factors for Nonalcoholic Steatohepatitis (NASH)

H Lee, K Dresser, EM Kurian. Albany Medical Center, Albany, NY; University of Massachusetts, Worcester, MA; University of Texas Southwestern Medical Center, Dallas, TX.

Background: Concomitant steatohepatitis in HCV hepatitis is associated with fibrosis, and decreases the likelihood of achieving a sustained virologic response. Central zone (CZ) injury in nonalcoholic steatohepatitis (NASH) manifests as central portalization (increased vascular channels and ductular reaction in the CZ). We hypothesize that central portalization in steatotic HCV biopsies would identify patients with risk factors for NASH.

Design: Clinical data and liver biopsies with HCV hepatitis and >10% steatosis (65) were compared to cases of steatohepatitis without HCV (22) and HCV hepatitis with ≤10% steatosis (20). The number of CZ showing arterioles, microvessel proliferation (MP), and ductular reaction (DR) was evaluated by the immunostaining for anti-smooth muscle actin (SMA), CD34, and CK7. The ratio of CZ harboring arterioles, MP, and DR versus total number of CZ were calculated.

Results:

Table 1

	Steatohepatitis, no HCV	HCV >10% steatosis	HCV ≤10% steatosis
Number of cases	22	65	20
NIDDM	5(22.7%)	14(21.5%)	1(5%)
Obesity	20(91%)	31(48%)	5(25%)
HCV genotype			
1a/1b	n/a	34(77.3%)	17(100%)
2a/2b	n/a	3(6.8%)	0
3	n/a	7(15.9%)	0
Steatosis			
<33%	10(45.5%)	22(33.8%)	20(100%)
33-67%	3(13.6%)	30(46.1%)	0
>67%	9(40.9%)	13(20%)	0

Obese patients (Body Mass Index≥30) showed less fibrosis (mean Ishak's stage 2.9) than those without obesity (mean Ishak's stage 3.9). The degree of fibrosis or steatosis did not differ between those with and without non-insulin dependent diabetes mellitus (NIDDM), history of alcohol use, and HCV genotype 3. The MP and DR showed positive correlation with fibrosis (r=0.38 and 0.36, p=0.0076 and 0.013 by Pearson's correlation test, respectively), however, did not identify patients with obesity, NIDDM, genotype 3 HCV, history of alcohol use, and history of treatment.

Conclusions: In steatotic HCV liver biopsies, over a half of the patients have one or more risk factors for NASH. Positive correlation of MP and DR with fibrosis indicates the role of central zone injury in the progression of fibrosis in this population. However, the central zone injury is not solely attributable to the risk factors for NASH or genotype 3 HCV. Further studies are needed to better understand the pathogenesis of steatosis and central zone injury in HCV hepatitis.

1737 Dialysis-Associated Hepatopathy: Histopathologic Resemblance to Noncirrhotic Portal Hypertension

H Lee, CE Sheehan, J Lin. Albany Medical College, Albany, NY; Indiana University, Indianapolis, IN.

Background: Hepatic pathology associated with dialysis is unknown. Liver biopsy performed on patients on dialysis may fail to reveal diagnostic features to explain clinical manifestations and necessitate repeat procedures. We reviewed liver biopsies from patients on dialysis to evaluate hepatic pathology associated with dialysis.

Design: Liver biopsies from patients on hemodialysis or peritoneal dialysis were retrieved (2000-2013). Relevant clinical history was obtained by review of medical records. H&E, reticulin, and CK7 stain were performed on the sections from paraffin-embedded tissue blocks. Original trichrome stains were reviewed.

Results: Thirteen liver biopsies were retrieved: 10 male, 3 female; mean age 55 (range 22-74) years; 12 hemodialysis and 1 peritoneal dialysis; mean cumulative duration of dialysis 50 months (range 17 months to 11 years). Three had history of failed renal transplant prior to dialysis. Comorbidities included hypertension (7), diabetes mellitus (5), congestive heart failure (5), hypercoagulability (4), HCV (4) and HIV (3). Indication for biopsy was a combination of abnormal liver function test (5), portal hypertension (3), ascites (3) and possible cirrhosis (3). Two patients with portal hypertension underwent multiple liver biopsies for diagnosis. Seven patients had selective elevation of alkaline phosphatase (range 146-484 IU/L). Ten biopsies showed portal vasculopathy including narrowed lumen (9), increased vascular channels (8), and shunt vessels (3). Megasinusoids (9), nodular regenerative hyperplasia (5), features of venous outflow obstruction (3) and clustered central veins (2) were also noted. Nine cases showed portal (4), periportal (3), and bridging (2) fibrosis. Five cases showed focal to extensive perisinusoidal fibrosis. No cirrhosis was identified. Portal and lobular inflammation was minimal to mild. Variable degree of bile ductular proliferation was noted.

Conclusions: Dialysis-associated hepatopathy demonstrates a spectrum of features of idiopathic noncirrhotic portal hypertension, including portal vasculopathy, nodular regenerative hyperplasia, and variable portal and perisinusoidal fibrosis, implying underlying vasculopathy as a potential culprit. Patients may present with portal hypertension, ascites or abnormal liver function tests. The etiology appears multifactorial in this population. Recognition of this pattern of injury in patients on dialysis will help to avoid unnecessary procedures or overdiagnosis of cirrhosis and chronic hepatitides.

1738 Clinicopathologic Features of Hepatocellular Carcinoma with Prominent Lymphoid Stroma

L Liang, A Rashid, J-N Vauthey, H Wang. The University of Texas Medical School at Houston, Houston, TX; The University of Texas MD Anderson Cancer Center, Houston, TX.

Background: Although tumor-infiltrating lymphocytes are found in conventional hepatocellular carcinoma (HCC), but it is unusual to see HCC with prominent lymphoid stroma. Given the rarity of this entity, the clinicopathologic features of HCC with prominent lymphoid stroma have not been examined in detail.

Design: Nine cases of HCC with prominent lymphoid stroma were identified in the electronic pathology database at our institution from 2002 to 2013. The slides from all cases were reviewed by two pathologists to confirm the diagnosis. The clinicopathologic and survival data were obtained by medical chart review.

Results: The patient age ranged from 51 to 82 years with the mean age 69 years and a male to female ratio 1.25:1. Among these patients, the clinical, radiological and follow up data were available in 7 patients. Hepatitis C and cirrhosis were present in 4 and 2 cases respectively. None of our cases had hepatitis B. Epstein-Barr virus (EBV) was tested by in situ hybridization in two patients and both were negative. Five patients presented with single tumor nodule and two patients presented with multiple tumor nodules. The size of largest tumor ranged from 1.7 to 13.0 centimeters.The patients were treated with resection (n=1), resection following hepatic artery chemoembolism (TACE, n=2), radiofrequency ablation (n=1), TACE and radiofrequency ablation (n=1), orthotopic liver transplantation (n=1), or chemotherapy only (n=1). During follow-up, three patients had no evidence of disease at 96, 78 and 12 months, two were alive with disease at 77 and 30.6 months, two died of disease at 82 and 5.8 months respectively and two patients were lost to follow up. The only patient who expired within 6 months following initial diagnosis, presented with multiple hepatic tumor nodules, and lymph node and adrenal gland metastasis that were unresectable and underwent chemotherapy only.

Conclusions: Our study showed that HCC with predominant lymphoid stroma were associated with high frequency of hepatitis C infection. Compared to conventional HCC which had a reported median survival of 6 to 20 months, HCC with predominant lymphoid stroma seems to show a better prognosis.

1739 SALL4 Immunoreactivity Predicts Prognosis in Western Hepatocellular Carcinoma Patients but Is a Rare Event – A Study of 236 Cases

T-C Liu, N Vachharajani, WC Chapman, EM Brunt. Washington University, St. Louis, MO.

Background: Prognostic biomarkers that stratify patients with cancer are needed. Recent studies from Asia have implicated SALL4, a stem cell marker, as useful in identifying aggressive cases of hepatocellular carcinoma (HCC). Given the differences in predominant etiologic factors between the Asian and Western HCC, we sought to determine the prevalence of SALL4 immunoreactivity and its clinical relevance in Western HCC patients.

Design: We constructed tissue microarrays from 236 adult HCC. Two cores each of tumor and nontumor tissue were included for each case. SALL4 immunohistochemistry was scored in a semi-quantitative manner and the results were correlated with recurrence-free and overall survival, in addition to standard demographics.

Results: Among the 236 cases, 165 (70.0%) were male. The median age was 59 years (range: 19-83 years). The majority (78.4%) of patients were Caucasian, followed by African American (15.7%), Asian (3.8%), Hispanic (1.7%), and Native American (0.4%). The majority of patients had hepatitis C (42.8%), followed by alcoholic liver disease and hepatitis B (both 8.9%), and nonalcoholic steatohepatitis (3.8%). SALL4 immunoreactivity was detected in a total of 3 cases (1.3%). By univariate analysis, the SALL4-positive cases had significantly higher tumor grade (p=0.0251), common lymphovascular invasion (p=0.0150), shorter recurrence-free survival (7.90 vs. 57.54 months; p = 0.0115) and overall survival (7.90 vs. 64.87 months; p = 0.0018).

Conclusions: While SALL4 immunoreactivity in Western HCC is correlated with higher grade and poor prognosis, this is a rare event. Therefore, universal application of SALL4 as a biomarker for HCC should be done with caution.

1740 Histologic Findings in Liver Biopsies from Patients Prior to Heart Transplant

CY Louie, N Kambham, T Daugherty, M Pham, JP Higgins. Stanford Hospital and Clinics, Stanford, CA.

Background: Liver biopsies may be performed in cardiac transplant candidates in an attempt to assess the degree of liver injury related to chronic passive congestion from heart failure. The findings on liver biopsy may be used to exclude the patient from undergoing transplant with a rationale that the risk of operative mortality may be too high to justify the transplant; however, the operative risk based on liver biopsy findings is not well established. We sought to characterize the histologic changes in liver biopsies in patients undergoing evaluation for heart transplant and to correlate the findings with clinical parameters and outcome after cardiac transplantation.

Design: We identified 27 liver biopsies from patients at our institution who subsequently received heart transplants over a 16 year period (1997-2012). 7 cases were excluded due to other causes of liver injury (viral hepatitis B and C). The remaining 20 biopsies were examined by H&E and trichrome stains. Histologic parameters examined included sinusoidal dilation, fibrosis (pattern and extent), presence of regenerative nodules, and necrosis. Clinical background and follow up was also obtained for each patient.

Results: Out of the 20 liver biopsies examined, all except 2 showed sinusoidal dilation and congestion (7 mild, 8 moderate, and 3 severe cases). Regenerative nodules were seen in 7 of the cases. Coagulative necrosis was not seen in any case. All biopsies except 2 showed increased fibrosis, in a bridging and/or pericellular distribution. The degree

of fibrosis was graded as mild (4 cases), moderate (12 cases), or severe (2 cases). Out of the biopsies classified as moderate or severe fibrosis, 12 showed bridging fibrosis. From these 12 cases, 2 patients clinically had prolonged liver failure post transplant, and 1 patient died within 2 months post-op, from causes related to right ventricular failure. Out of the 6 cases with mild or no fibrosis, one patient died within 2 months post-op, from respiratory and right heart failure.
Conclusions: The majority of the cases showed at least mild fibrosis, and most cases showed moderate to severe fibrosis. Almost all the patients with moderate or severe and bridging fibrosis survived the immediate post-op period (at least 2 months), with only 2 patients showing prolonged liver failure post transplant. One patient showing mild fibrosis died in the immediate post-op period. Overall, post-operative mortality was low regardless of the fibrosis seen pretransplant. The findings support that moderate to severe fibrosis on liver biopsy does not, per se, indicate a poor outcome following cardiac transplantation.

1741 Characterization of the Immune Response in Pediatric Acute Liver Failure of Unknown Etiology

CY Louie, R Mckenzie, RK Sibley. Stanford Hospital and Clinics, Stanford, CA.
Background: The host immune response is a frequent mediator of cellular injury in the context of liver disease. A number of severe acute liver failure cases in children requiring liver transplant are of unknown etiology; the composition of the inflammation in these cases has been largely undescribed. We sought to characterize the inflammatory response in pediatric acute liver failure cases of unknown etiology, as further characterization may reveal causative factors or suggest targets of immunomodulatory therapies in these difficult cases.
Design: The immune response in 11 liver explants and biopsies from pediatric patients with liver failure of unknown etiology was compared to 10 pediatric liver cases with definitive diagnoses (4 autoimmune hepatitis, 3 Wilson's disease, and 3 drug-induced hepatitis). The cases were examined with H&E and immunohistochemical stains for CD3, CD20, CD4, CD8, and cytotoxic markers including T-bet, TIA-1, granzyme, and perforin. Lymphocytes were enumerated on each stain per high-powered field in portal tracts and lobules. Additionally, ratios were determined including CD3:CD20 and CD8:CD4.
Results: The cases of unknown etiology showed CD3:CD20 in portal tracts and lobules ranging from 1.5:1 to 200:1, with some cases showing a marked predominance of T cells. In contrast, the 10 cases of known etiology showed ratios ranging from 3:1 to 20:1. Most of the unknown cases (8/11) and autoimmune cases (3/4) showed CD8:CD4 of >10:1 in the lobules, indicating a CD8+ T cell predominance; in comparison, the drug and Wilson's disease cases showed lobular CD8:CD4 of <10:1. In portal tracts, most cases showed CD8:CD4 of <10:1 (10/11 unknown, 3/4 autoimmune, 3/3 drug, 3/3 Wilson's cases), indicating that the unknown cases had a higher proportion of T cells in lobules than in portal tracts. 8/11 of the unknown cases showed positive staining for at least one of the four cytotoxic T-cell markers in >10 cells per high-powered field.
Conclusions: The 11 cases of acute liver failure of unknown etiology all showed T cell infiltrates, with most of the cases showing that the majority of the T cells in lobules are CD8+ and express cytotoxic markers. The unknown cases showed an immune composition similar to the autoimmune hepatitis cases, suggesting a related mechanism of inflammatory cell mediated damage and possibly providing a rationale for immunomodulatory therapy. T cells have also been shown to mediate cell damage in viral hepatitis; the findings also lend support to the hypothesis that acute liver failure of unknown etiology may be triggered by viral causes.

1742 Lack of Histological Significance of Antinuclear Antibodies in Patients with Nonalcoholic Fatty Liver Disease (NAFLD)

HR Makhlouf, G Giblen, DE Kleiner, ZD Goodman. National Cancer Institute, National Institutes of Health, Bethesda, MD; Mercy Medical Center, Baltimore, MD; Inova Fairfax Hospital, Falls Church, VA.
Background: There is a high frequency of autoantibodies in patients with non-alcoholic fatty liver disease (NAFLD) with about 20% of patients having anti-nuclear antibodies (ANA) and a few percent with antibodies to smooth muscle actin. Autoantibodies may cause diagnostic confusion between NAFLD and autoimmune hepatitis. Previous studies have not identified clinically significant differences in histology in ANA-positive patients, but features of chronic hepatitis or plasma cell infiltrates have not been examined in detail.
Design: The files of the AFIP were searched for cases of NAFLD in which ANA results were available. These were blindly scored for features of chronic hepatitis (Ishak) and NAFLD (NASH CRN). In addition, the degree of plasma cell infiltrates, portal fibrosis, perisinusoidal fibrosis and bridging fibrosis were scored from 0 to 3 (none, mild, moderate, marked). Statistical analysis used Chi-square and Mann-Whitney U tests.
Results: 136 biopsies were available for review. The mean age of the patients was 51 (range 13-81) years and 67% were female. 56 patients (41%) had positive ANA results, probably reflecting referral bias. Women were more likely than men to have a positive ANA result ($p = 0.006$). There were no discernible differences in features of chronic hepatitis or NAFLD using the standard scoring systems. Plasma cell infiltrates were present in 65% of biopsies. However, there were no significant differences in plasma cell infiltrates or in the various fibrosis categories between patients with circulating ANA and those without.
Conclusions: Although autoantibodies are a frequent finding in patients with NAFLD, we were unable to demonstrate histological differences in cases of NAFLD between patients with and without circulating ANA.

1743 Hepatic iNOS Expression Correlates with Hepatitis C Progression in Liver Transplant Recipients and Hepatocarcinogenesis

L Mei, B Rea, KM Choi, R Chennuri, A Quintana, A Chan, G Guzman. University of Illinois at Chicago, Chicago, IL; University of Pennsylvania, Philadelphia, PA; New York University, New York, NY.
Background: Hepatitis C virus (HCV) infection is the most common cause of cirrhosis, a major risk factor for hepatocellular carcinoma (HCC) and the leading indication for liver transplantation. HCC in the setting of HCV likely evolves through a continuum of inflammation, cirrhosis, dysplasia and carcinoma; however the molecular mechanism is unclear. Post-transplant HCV recurrence is nearly universal but varies in rapidity. There is evidence that oxidative stress plays a key role in HCV progression and carcinogenesis, and the expression of the inducible nitric oxide synthase (iNOS) gene is increased in chronic HCV patients. We investigated the association between nitrosative stress and post-transplant HCV recurrence using iNOS expression as a marker. We further examined the role of nitrosative stress in HCV progression by characterizing the relationship of iNOS expression level with pre-cancerous lesions, HCC, and other biomarkers (8-OHdG and HK2).
Design: 57 liver biopsies were obtained from 28 patients with HCV re-infection after liver transplantation. A liver pathologist, blinded to clinical data, retrospectively scored the hepatitis activity index (HAI) using the Batts and Ludwig criteria. A liver tissue microarray (TMA) was also constructed containing 8 normal controls and 45 subjects with cirrhosis, dysplasia and HCC. Standard IHC staining was performed. Immunostaining of the TMA slides was quantified by digital imaging.
Results: In post-transplant HCV recurrence, high intensity iNOS staining was associated with higher grade of hepatic inflammation, higher stage of fibrosis, higher HAI score and more rapid progression to bridging fibrosis or cirrhosis. On the TMA, iNOS expression was significantly increased in HCC compared to cirrhosis. iNOS also strongly correlated with HK2, a marker of cellular metabolism. Increased expression of iNOS and HK2 was associated with higher HCC stages. Poorly differentiated tumors showed higher expression of HK2 and 8-OHdG, a marker of oxidative stress. Finally, pleomorphic type HCC displayed higher levels of iNOS and HK2 than other histologic types.
Conclusions: Hepatic iNOS expression correlates with HCV progression and hepatocarcinogenesis. It is also associated with other biomarkers of cellular metabolism and oxidative stress. These results indicate that iNOS expression may have prognostic and clinical significance in HCV and HCC.

1744 Liver Carcinogenesis Related to Metabolic Syndrome: Metformin as a New Therapeutic Tool

M Mouniya, B Lotfi, P Valerie, B Pierre. INSERM, Clichy, France; Department of Pathology, Clichy, France.
Background: Metabolic syndrome (MS) is becoming the leading cause of chronic liver diseases worldwide and may result in the development of Non-Alcoholic Fatty Liver diseases (NAFLD) including steatosis, steato-hepatitis (NASH) and fibrosis. In that context, type 2 diabetes and obesity are independent risk factors for hepatocellular carcinoma (HCC) development. Metformin, a biguanide widely used to treat type 2 diabetes, has been shown to decrease HCC risk in large epidemiological studies. The objective of this study was to evaluate the antitumor effects of metformin in HCC.
Design: Antineoplastic effects of metformin (5, 10 and 15 mM) on cell viability (MTT), proliferation (Brdu), apoptosis (caspase 3 expression) and cell cycle were studied in human hepatoma cell lines (HepG2, Huh7 and Hep3B). Effects were also investigated in presence of metformin in association with sorafenib (1 μM) and everolimus (0.1 μM). Expression profile of mTOR, p70S6K and 4EBP1 phosphorylated forms was assessed by western blot. To evaluate preventive effect of metformin in *in vivo* model of liver carcinogenesis, ($1x10^7$) HepG2 cell were injected subcutaneously, all mice developed tumours in 15 days. Mice were randomly distributed into each group, untreated or treated by 200 mg/kg of metformin. Xenograft tumours were resected after 54 days of observation.
Results: Antiproliferative effect of metformin was observed in all cell lines whatever the concentration tested (40 to 70% decrease, with a maximal effect in HepG2); the same effect was observed in combination metformin with sorafenib and metformin with everolimus. Whereas a low apoptotic effect was observed in presence of metformin alone in HepG2 and HuH7 cells, significant induction of apoptosis was observed in presence of metformin, sorafenib and everolimus. Expression of phosphorylated, mTOR, p70S6K and 4EBP1 as its downstream effectors, was decreased in cells treated with Metformin compared to control and cells treated with Sorafenib, it decreased significantly in cells treated with the combination of Met + Sora and Met +Evero. Metformin use in diabetic patients is associated with a decreased risk for HCC development; our *in vivo* experiments showed a significant decrease in the size of treated tumors.
Conclusions: Our findings indicate that metformin is effective at initiating apoptosis and inhibiting HCC cells proliferation. These effects were more important when we associate metformin with different drugs. Also metformin accelerates HCC regression in a xenograft model.

1745 Direct Demonstration of Fusion Products of Donor Cells and Recipient Hepatocytes in Human Hematopoietic Cell Transplant Recipients; and Statistical Analysis Suggesting Fusion Is the Only Mechanism Producing Donor Associated Hepatocytes

D Myerson, RK Parkin. Fred Hutchinson Cancer Research Center, Seattle, WA.
Background: Reconstitution of hepatocytes by hematopoietic stem cells has been observed in rodent experimental systems under highly selective conditions. Fusion between incoming myelomonocytes and host hepatocytes, with subsequent proliferation, is the mechanism. In human hematopoietic stem cell transplant recipients, greater frequencies of marrow derived hepatocytes have been demonstrated, but technical

artifacts are the suspected explanation. We created a highly specific conjoint immunohistochemistry–*in situ* hybridization technique to evaluate donor-associated hepatocyte nuclei, and a statistical modeling approach to determine accurate frequencies of various products.

Design: We studied liver tissue of female hematopoietic cell transplant recipients, 4 with male donors, and 5 as controls with female donors. We quantified the donor contribution under light microscopy on a single formalin-fixed paraffin-embedded section. Hepatocytes were identified by morphology and Cam 5.2 staining, and all nuclei were evaluated for X and Y chromosome content. We developed a model based on the binomial distribution assuming the probability of X (or Y) detection was the same for each instance of signal. Models were created to account for normal hepatocyte tetraploidy, and the fusion products of male cells with female hepatocytes.

Results: 1,640,000 hepatocyte nuclei were evaluated from female hematopoietic transplant recipients with male donors. They showed 350,900 [0] (without a sex chromosome), 805,400 X, 437,500 XX, 37,800 XXX, 8,400 XXXX, 1 Y, 34 XY, 26 XXY, 6 XXXY, and no YY, XYY, or XXYY. It is evident by inspection that only fusion can produce the observed mixed tetraploid XXXY, directly observed at a frequency of 4 per 10^6 hepatocytes. Directly observed normal female tetraploids XXXX averaged 0.5%. X and Y content in the nuclei were compared to the predicted distribution. The resulting fit gave robust frequencies for normal female tetraploidy XXXX, 8.3%, and fused mixed tetraploids XXXY, 80 per 10^6.

Conclusions: Only mixed tetraploids and their truncation products were directly demonstrated, indicating fusion as the mechanism. No male tetraploids or their specific truncation products were detected, refuting any evidence of transdifferentiation. We found and photographed 6 XXXY "mixed" tetraploids. We developed a binomial model that suggests that all the Y containing cells can be explained as the result of fusion.

1746 Prognostic Value of c-MET and CA9 Tumoral Expression in Hepatocellular Carcinoma (HCC)

V Paradis, A Tijas-Raballand, M Albuquerque, C Neuzillet, F Bladt, C Ihling, M Klevesath, H Zheng, E Raymond, A De Gramont, P Bedossa, S Faivre. Beaujon Hospital, Clichy, France; Inserm U773, Clichy, France; AAREC Filia Research, Clichy, France; Merck KGaA, Darmstadt, Germany; EMD Serono, Billerica, MA; Inserm U728, Paris, France.

Background: Prognosis of patients with HCC is mainly based in practice on clinico-pathological criteria. Increasing studies highlighted the additional prognostic value of molecular features. Next step would be to identify biomarkers predictive of response to targeted therapies. In addition to antiangiogenic drugs, other pathway inhibitors, including cMET inhibitors, have been developed. The aim of this study was to correlate c-MET and CA9 liver expression by immunochemistry with clinicopathologic data and disease-free survival (DFS) in patients with HCC.

Design: 100 HCC cases surgically resected were studied by immunohistochemistry (anti-c-MET clone Sp44 Ventana and polyclonal CA9 Novus Biological). Staining results were qualitatively and quantitatively assessed (using manual and automated evaluation) and correlated with clinicobiologic parameters. High c-MET expression was defined as moderate to strong (2+ and 3+ on a 0-3+ scale).

Results: HCC were classified as BCLC A1 (92%), uninodular (53%), low-AFP-expressing (81%), moderately-differentiated (60%), and with vascular invasion (70%). High c-MET expression was observed in 51% of HCC. c-MET expression was higher in patients with viral hepatitis-associated HCC (p=0.02) and with AFP>400UI/L (p=0.03). High CA9 expression was observed in 41% of HCC, correlated with viral hepatitis (p=0.002), vascular invasion (p=0.007), and poor differentiation (p=0.007). c-MET and CA9 expression significantly correlated with each other (p=0.008). Median DFS was shorter in high- compared to low-c-MET (12.9 vs 80 months, p=0.018) and high-CA9 compared to low-CA9 (10.2 vs 34.4 months, p=0.02) patients. c-MET and CA9 status discriminated 4 prognostic groups: poor (c-MET-high/CA9-high median DFS 10.7 months), intermediate (c-MET-high/CA9-low and c-MET-low/CA9-high, 10<median DFS<29 months), and good (c-MET-low/CA9-low, median DFS not reached), p=0.003). Multivariate analysis showed that tumor size (p=0.025), morphology (p=0.004), and CA9 expression (p=0.007) were independently associated with DFS; c-MET expression level was associated with DFS when CA9 was excluded from the model (p=0.024).

Conclusions: c-MET and CA9 are new prognostic markers of HCC. Analysis of c-MET expression in HCC might be helpful for selecting patients who potentially benefit from therapy with c-MET inhibitors.

1747 Estimation of Liver Collagen Proportionate Area by Visual Inspection

M Pavlides, LM Wang, E Fryer, DW Delaney, N Sarania, R Banerjee, S Neubauer, E Barnes, KA Fleming. University of Oxford, Oxford, Oxfordshire, United Kingdom; Oxford University Hospitals, Oxford, Oxfordshire, United Kingdom.

Background: The quantification of collagen as a proportion of the total liver biopsy area (Collagen Proportionate Area;CPA) using digital imaging analysis (DIA) has been proposed as an improvement to fibrosis assessment using categorical scores. In this study we assessed the performance of CPA estimation by visual inspection (visual-CPA) against CPA analysis by DIA (DIA-CPA) as the reference standard.

Design: Sixty five unselected liver biopsy slides were independently assessed by 3 tertiary centre pathologists who estimated visual-CPA using a standard light microscope. In 48 slides stained with Sirius Red, Image J was used for DIA-CPA. The associations between the visual-CPA and DIA-CPA were assessed using Pearson's correlation and linear regression. The inter-observer variability of visual-CPA (n=65) and DIA-CPA (n=20, scored by 2 further pathologists) was assessed by calculation of the concordance co-efficient.

Results: DIA-CPA (n=48; analysed by pathologist 1) correlated strongly with Ishak staging (r_s=0.84, p<0.0001). In 20 samples analysed using DIA by 2 further independent pathologists the concordance co-efficients were (0.94 vs Pathologist 2; 0.93 vs Pathologist 3; 0.94 for Pathologist 2 vs Pathologist 3). There was a highly significant association between DIA-CPA and visual-CPA for each of the 3 pathologists and the mean of the three estimates (r=0.90, R^2=0.80 for pathologist 1; r=0.91, R^2=0.84 for Pathologist 3; r=0.86, R^2=0.74 for Pathologist 4; r=0.94, R^2=0.88 for the mean of the 3 pathologists).

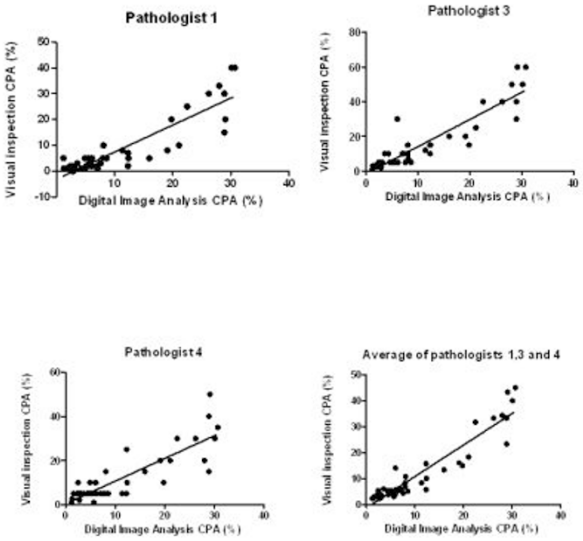

The concordance co-efficients for visual-CPA assessment were (0.71 for pathologist 1 vs pathologist 3; 0.74 for pathologist 1 vs pathologist 4; 0.71 for pathologist 3 vs pathologist 4).

Conclusions: Collagen proportionate area estimation by digital imaging analysis is highly reproducible as shown by the high concordance co-efficients achieved here. However, for the purposes of routine clinical practice, CPA by visual inspection may be sufficient as this method achieves high correlation with DIA-CPA.

1748 Serum Amyloid A Immunohistochemical Staining Patterns in Hepatitis

KC Piotti, RK Yantiss, Z Chen, J Jessurun. Weill Cornell Medical College, NY, NY.

Background: Serum amyloid A (SAA) is an acute phase reactant that is produced in hepatocytes. Protein levels are often elevated in the serum of patients with inflammatory and neoplastic diseases, leading some to hypothesize that SAA plays a role in host defense. Indeed, this protein may have antiviral activity against hepatitis C virus (HCV). SAA immunostains are also helpful in the classification of hepatocellular neoplasms, as the protein is expressed in inflammatory adenomas but not other lesions. For this reason, SAA immunohistochemistry is increasingly used in needle biopsies of hepatic tumors, although the specificity of this marker for inflammatory adenomas has not been confirmed. We performed this study to assess SAA staining in inflammatory conditions of the liver.

Design: We performed SAA immunostains on 160 medical liver biopsy specimens, including 100 cases of HCV infection with stage 0, 1, 2, 3, and 4 fibrosis (20 cases of each), 20 cases of hepatitis B viral infection, 20 cases of steatohepatitis, and 20 cases of autoimmune hepatitis. Extent and location of staining was recorded and correlated with inflammation grade, fibrosis stage, and laboratory values (AST, ALT, bilirubin, viral load). Data were analyzed using the Cochran-Mantel-Haenszel Chi-square test for trend.

Results: Positive staining was present in 130 (81%) cases and was most pronounced in zone 3 perivenular hepatocytes. Biopsies with less inflammation and fibrosis showed more SAA staining than those with more active hepatitis and/or cirrhosis (p<0.001, all comparisons). An inverse correlation with transaminase levels was present: less SAA staining was seen in biopsies from patients with elevated AST or ALT (p<0.001, both comparisons). There was no significant association with lobular inflammation (p=0.056), bilirubin or viral load.

Conclusions: SAA immunopositivity is common in biopsies with mildly active chronic hepatitis and early stage fibrosis, supporting the notion that SAA is primarily expressed in early phases of disease. This marker is often present in patients with known liver disease and normal transaminase levels, suggesting that SAA is an early marker of hepatocyte damage. Prospective studies correlating SAA staining in liver cells with prognosis and/or response to therapy may be warranted. From a practical standpoint, SAA is not a specific marker of inflammatory adenoma in liver biopsy material and care must be taken to ensure that positive staining is observed in lesional tissue rather than inflamed hepatic parenchyma.

1749 Altered Expression of MiR-21, MiR-27b, MiR-10b and MiR-146a in Different Stages of Nonalcoholic Fatty Liver Disease

J Putra, FB de Abreu, PR Burchard, A Toor, GJ Tsongalis, AA Suriawinata. Dartmouth-Hitchcock Medical Center, Lebanon, NH; Dartmouth College, Lebanon, NH.

Background: MicroRNA (miR), a non-protein-coding RNA that regulates gene expression, has been shown to play a role in the pathogenesis of nonalcoholic fatty

liver disease (NAFLD). In this study, we evaluated the expression of several miRs in different stages of NAFLD (steatosis and steatohepatitis) in order to identify potential new diagnostic biomarkers and novel therapeutic targets.

Design: Two study groups comprised of 14 steatohepatitis patients (71% female, age 50 ± 8.7 years, BMI 37 ± 5.4) and 14 patients with steatosis (85% female, age 51 ± 4.7 years, BMI 45 ± 8.3) were selected from a list of patients who underwent liver biopsy prior to or during bariatric surgery at our institution (2006-2012). Fourteen patients from the same list who had normal liver biopsies were chosen as the control group (64% female, age 49 ± 11.4 years, BMI 44 ± 13.3). Expression of miRs was evaluated on formalin-fixed paraffin embedded tissue sections using qRT-PCR. Total RNA extraction was performed using the Qiagen miRNeasy FFPE Kit. Reverse transcriptase reactions were carried out using the TaqMan® MicroRNA Reverse Transcription Kit (Applied Biosystems) with primers specific for the following miRNAs: RNU6B (internal control), miR-21, miR-27b, miR-10b and miR-146a. Real time PCR reactions were performed on the AB 7500 Fast Real-Time PCR System. Each PCR reaction was run in duplicate with the internal control. The average cycle threshold (C_q) value was calculated and used to determine expression levels of each miR ($2^{-\Delta\Delta Cq}$).

Results: Our data showed that miR-146a and miR-27 levels were underexpressed in 80% steatosis cases and 100% steatohepatitis cases. MiR-146a levels in steatohepatitis group were shown to be lower than in steatosis group (~3Cq difference). Meanwhile, miR-27 expression was lower in steatohepatitis group (~3Cq difference). Both study groups (100% of steatosis and steatohepatitis cases) also showed an increase in miR-10b expression level. Additionally, miR-21 was overexpressed in 93% steatosis cases and 57% steatohepatitis cases.

Conclusions: The study shows altered miR-21, miR-27b, miR-10b and miR-146a expression in patients with steatosis and steatohepatitis. Furthermore, we found different expression levels of miR-146a and miR-27 in steatosis and steatohepatitis. The findings may be associated with the disease progression and could be useful as a diagnostic marker to distinguish different stages of NAFLD.

1750 Evaluation of Fibrosis in Serial Liver Biopsies of Nonalcoholic Fatty Liver Disease: Is FIB-4 Score as Good as Liver Biopsy?

J Putra, LM Glass, A Toor, AA Suriawinata. Dartmouth-Hitchcock Medical Center, Lebanon, NH.

Background: FIB-4 score, a noninvasive marker for staging fibrosis in chronic hepatitis C, has been reported to be reliable in excluding advanced fibrosis in patients with nonalcoholic fatty liver disease (NAFLD). This is the first study, to our knowledge, to demonstrate the diagnostic value of this scoring system in serial liver biopsies of NAFLD patients. We investigated the reproducibility of FIB-4 score in initial and repeat biopsies in our institution.

Design: Thirty-eight NAFLD patients who underwent serial liver biopsies (1-7 year intervals) from 2002-2011 were selected for the study. 73% of the patients were female and the average age at the time of initial biopsy was 47 years. Fibrosis staging was based on the Nonalcoholic Steatohepatitis Clinical Research Network criteria (stage 0-4). Cases were further classified into 2 groups: low-stage fibrosis (stage 0-2) and advanced fibrosis (stage 3-4). FIB-4 score (age x AST (IU/l)/ [platelet (10^9/l) x □ALT (IU/l)]) at the time of each biopsy was calculated. A score of 1.3 was predetermined as the cutoff point based on previous studies with similar patient population. FIB-4 score below the cutoff point was indicative of low-stage fibrosis. Statistical analysis of the scoring system at the time of initial and repeat biopsies was compared to determine its reproducibility.

Results: The frequency of advanced fibrosis in initial and repeat biopsies was 42.2% and 23.7% respectively. FIB-4 score of < 1.3 was highly reliable to exclude patients with advanced fibrosis at the time of repeat biopsies with negative predictive value (NPV) of 90.4%. However, it only showed moderate value during the initial biopsies (NPV: 57.6%). Almost half (42.3%) of patients with advanced fibrosis were mischaracterized using FIB-4 score at the time of first liver biopsy. Test characteristics for initial and repeat biopsies are shown in Table 1.

	Initial biopsies (n=38)	Repeat biopsies (n=38)
Sensitivity	31.2%	77.7%
Specificity	68.2%	65.6%
PPV	41.6%	41.1%
NPV	57.6%	90.4%

PPV = Positive predictive value; NPV = Negative predictive value

Conclusions: Our study showed that FIB-4 score was noticeably inconsistent in excluding NAFLD patients with advanced liver fibrosis. A significant number of patients with advanced fibrosis would not have been detected if they were solely tested with the aforementioned scoring system. Liver biopsy remains the preferred diagnostic method to evaluate fibrosis in NAFLD patients.

1751 Involvement of Intracellular Domain of EpCAM in Hepatocellular Carcinoma

E Sahin, D Nart, I Kunter, E Kandemis, F Yilmaz Barbet, N Atabey, E Erdal. Faculty of Medicine, Dokuz Eylul University, Izmir, Turkey; Faculty of Medicine, Ege University, Izmir, Turkey.

Background: The heterogeneous nature of hepatocellular carcinoma (HCC) and the lack of appropriate biomarkers limit patient prognosis and treatment strategies. Epithelial cell adhesion molecule EpCAM is a transmembrane glycoprotein, which is frequently over-expressed in epithelia, progenitors, embryonic and tissue stem cells, carcinoma and cancer-initiating cells. EpCAM+ cells, isolated from primary HCC and cell lines, show cancer stem cell features. However, little is known on how EpCAM+ cells regulate HCC progression. Recently, it was found that EpCAM requires intramembrane proteolysis for the activation of its signal transduction capacity. Upon cleavage, the extracellular domain EpEX is released as a soluble ligand while the intracellular domain EpICD translocates into the cytoplasm and eventually into the nucleus and drives cell proliferation as well as pluripotency.

Design: Expression of EpICD was assesed by immunohistochemical staining using specific antibody (clone E144) in 52 primary HCC tissues, 10 cirrhotic and 17 dysplastic nodules. A total immunostaining score for intensity and extensity were evaluated. Localization of EpICD was also analysed in all samples. Furthermore, EpCAM+ subpopulation has been isolated from a HCC cell line, Huh-7 by using magnetic separation, then used to analyse in vitro cell proliferation and tumorogenesis capacities by using real time proliferation assay by Xcelligence and sphere formation assay in matrigel, respectively.

Results: Herein we showed that nuclear and/or cytoplasmic EpICD is significantly high in both cirrhotic and dysplastic nodules (n=26) in comparison to HCC tumor samples (n=52), and was the most abundant in high grade dysplastic nodules (HGDN) among all tissue samples. Since HGDN is accepted as early HCC, we hypothesized that EpCAM signaling accompanying by EpICD translocation may be important in tumor initiation. Then we found that although EpCAM+ cells had significantly less proliferation ability, they formed spheres in matrigel with a larger diameter in comparison to EpCAM- cells.

Conclusions: The release of intracellular domain of EpCAM can be used as an early diagnostic marker in HCC and it may provide opportunities to develop new targets for HCC treatment.

1752 Histologic Spectrum of Bile Duct Injury in Prolonged Cholestatic Drug Reaction

SN Salaria, C Shi, K Washington. Vanderbilt University, Nashville, TN.

Background: Cholestatic drug induced liver injury (DILI) is associated with many pharmacologic agents, most commonly antibiotics. Inadequate clinical information, lag between antibiotic administration and biopsy make diagnosis difficult. We examined a series of 19 cases to determine the spectrum of bile duct injury (BDI) seen in DILI with prolonged cholestasis and correlated with clinicopathologic findings. We hypothesize that lack of bile ductular reaction (BDR) in these cases is due to inactivation of hepatic stem/progenitor cells (HPC).

Design: A pathology database search (1991-present) for cases of DILI, revealed 29 cases (19 males). They were evaluated for cholestasis, BDI, bile duct loss, BDR, and lobular injury. Patient records were reviewed for pertinent history, including time to resolution of liver test abnormalities. CD44, CD117, CK7 immunohistochemistry was used to visualize HPCs, bile duct morphology, & BDR.

Results: The mean age of the patients was 42 years; all presented with jaundice & malaise. Clinical history was available for 15 patients; 14 had no other hepatic disease, 1 had a complicated cholecystectomy. 3 patients had non-hepatic malignancies, of these 2 died of their disease (1 week to 3 years after liver biopsy from infections and cancer relapse, respectively). Pharmacologic history was available on 23 patients. 14 patients were taking antibiotics, 3 were taking steroids, & 4 were on a combination of antibiotics and steroids. Of those taking antibiotics 4 patients were taking amoxicillin/clavulanic acid and macrolides respectively, 2 were on antifungals, 1 on tetracycline & 3 patients were on a combination of antibiotics. Symptoms began 5 days to 3 weeks after exposure. The liver labs were elevated; total bilirubin (TB) at initial liver biopsy ranged 1.6-29.5 mg/dl. Resolution was gradual, averaging 19 months (range 0.1-96 months). TB at the last clinic visit ranged 0.3-22.1 mg/dl. Histopathology showed portal tract inflammation with infiltration of interlobular bile ducts by neutrophils and lymphocytes, and prominent centrilobular cholestasis. BDI ranged from active bile duct damage to ductopenia, with a uniform lack of BDR. CK7 showed minimal BDR in 2 specimens. Scattered CD117 and CD44 positive cells were noted at the limiting plate, as in normal portal tracts.

Conclusions: A spectrum of BDI ranging from mild infiltration by inflammatory cells, to prolonged ductopenia is encountered in DILI due to antibiotic therapy. BDR is not prominent in these cases, and HPCs are not increased. Clinical and biochemical resolution takes months to years.

1753 Expression of the Iron-Regulating MicroRNA miR-485-3p in Hepatic Cirrhosis

C Sangokoya, A Mattis, R Ramachandran, J Baron. University of California, San Francisco, San Francisco, CA.

Background: Hepatic iron accumulation is associated with the pathogenesis in chronic liver disease and correlates with resistance to therapy. However, the molecular mechanisms of dysregulated hepatic iron accumulation remain unknown. Ferroportin is the only known cellular iron exporter in mammalian cells and plays a critical role in both cellular and systemic iron balance. Recent findings reveal that the microRNA miR-485-3p directly targets ferroportin protein expression in human cells, suggesting a role for this microRNA in cellular iron homeostasis. This study aims to further characterize this microRNA in the human liver and cirrhotic liver disease.

Design: Paraffin-embedded formalin-fixed liver tissue samples from 46 patients who underwent liver biopsy or explantation (males n=28, females n=18, no significant pathologic abnormality n=10, non-viral cirrhosis n=11, Hepatitis B cirrhosis n=3, Hepatitis C cirrhosis n=22) were examined for expression of microRNA and RNA of known factors in liver cellular iron regulation. Immunohistochemical staining for ferroportin and special stains were performed and evaluated, with iron scoring performed independently by two pathologists.

Results: Compared to nonviral liver cirrhosis, miR-485-3p was significantly increased by 4.3-fold (p=.033) in Hepatitis C cirrhosis. This expression is prominent (5.2-fold increase, p=0.04) at low iron scores (0-1 out of 4). There were no significant changes in hepcidin, transferrin receptor, ferritin-light-chain, or ferroportin messenger RNA levels in Hepatitis C cirrhosis compared to non-viral cirrhosis, however, differential ferroportin protein expression is identified. In Hepatitis B cirrhosis, both miR-485-3p and hepcidin RNA levels were significantly increased.

Conclusions: In this study, we identify significantly elevated expression of miR-485-3p from human liver tissue with Hepatitis B and Hepatitis C cirrhosis compared to those with non-viral cirrhosis. In the Hepatitis C samples, miR-485-3p expression does not appear to be a secondary effect of altered cellular iron levels, evidenced by the non-significant changes in RNA expression of regulators important in iron homeostasis. We look to further characterize the relationship between miR-485-3p and ferroportin expression in hepatocyte parenchyma. These findings may be of clinical utility in the identification of miR-485-3p as a target for therapeutic regulation of liver iron in chronic liver disease.

1754 Liver Carcinogenesis Related to Metabolic Syndrome: Role of Fatty Acid-Binding Protein 4

A Sannier, S Laouirem, M Mebarki, M Albuquerque, P Bedossa, V Paradis. Inserm U773, Beaujon Hospital, Clichy, France, Metropolitan; Beaujon Hospital, Clichy, France, Metropolitan.

Background: Metabolic syndrome (MS) is a major risk factor for hepatocellular carcinoma (HCC), but the specific molecular pathways of tumorigenesis are incompletely understood. Plasmatic Fatty Acid-Binding Protein 4 (FABP4) levels, a mediator of lipid trafficking in adipocytes, are increased in patients with MS and correlated with lesions of steatohepatitis, suggesting a potential role for FABP4 in liver pathogenesis related to MS. In addition, some studies have shown that FABP4 may have an oncogenic potential. The aim of our study was to investigate FABP4 liver expression and its role in liver carcinogenesis related to MS.

Design: FABP4 expression was investigated by Western Blot, immunohistochemistry and RT-PCR on human HCCs and non tumoral liver samples related to MS, and compared with samples from patients having Hepatitis C Virus (HCV) chronic liver disease. FABP4 expression and its regulation were then studied in vitro on HCC (HepG2) and endothelial cell lines (HUVEC).

Results: FABP4 expression was significantly upregulated in HCCs related to MS compared with HCCs associated with HCV infection (4-fold, p=0.01). FABP4 expression was inversely correlated with the number of tumoral nodules and vascular invasion in HCCs related to MS. In patients with MS, FABP4 expression was increased in tumor samples compared with non tumoral samples (4-fold, p<0.01). Using double staining immunohistochemistry, FABP4 expression in HCC samples was restricted to endothelial cells. At baseline no FABP4 expression was detected in HepG2 and HUVEC. However, FABP4 expression was induced when endothelial cells were incubated in presence of insulin (1μM). In presence of FABP4, decreased cell proliferation was observed in HepG2 cell lines.

Conclusions: In MS, FABP4 upregulation is observed in HCCs, restricted to endothelial cells. These data suggest the potential relationship between endothelial and tumoral cells in HCCs via FABP4 upregulation.

1755 Intraductal Tubulo-Papillary Neoplasms of the Bile Ducts: Clinicopathologic and Immunohistochemical Analysis of 19 Cases

AM Schlitter, K-T Jang, B Saka, H Choi, GJ Offerhaus, R Hruban, Y Zen, S-M Hong, B Konukiewitz, M Allgauer, I Esposito, G Kloppel, M Reid, V Adsay. TUM, München, Germany; SMC, Seoul, Korea; EU, Atlanta, GA; UMC, Utrecht, Netherlands; JHU, Baltimore, MD; KCH, London, United Kingdom; AMC, Seoul, Korea.

Background: In the pancreas, intraductal tubulopapillary neoplasm (ITPN) is now a well-established category, also recognized by WHO in 2010. Its biliary counterpart is poorly characterized. Recently, Katabi et al presented 9 examples of this entity (AJSP, 2012;35:1647-1655) under the heading of "intraductal tubular neoplasms".

Design: 19 biliary intraductal neoplasms composed almost exclusively of non-mucinous tubular units with/without sheet-like growth, with no or minimal abortive papilla formation, occurring in extra- and intrahepatic bile ducts, were analyzed. Cases with overt papillary growth or mucinous pyloric gland pattern and/or MUC5AC expression were excluded.

Results: Clinical data: Mean age 64 (42-82); F/M = 1.6. Mean size = 6.1 cm (1.5-15). Intrahepatic 63%, extrahepatic 16%, and perihilar 21%. **Pathology**: In addition to characteristic tubular pattern: solid/poorly formed 68%, abortive papillae 47%, clear-cell parathyroid-like areas 16%, luminal calcifications/psammoma-bodies 16%, acidophilic secretions creating thyroid follicular pattern 11%, oncocytoid cytology 11%, focal spotty necrosis 42%, necrosis with "comedocarcinoma-like pattern" 37%, extensive necrosis 11%, and hyaline globules 11% were observed. **IHC:** MUC1 expression was common (79%) while MUC6 was less common (32%). MUC2 was not expressed. p53 was uncommon and focal (17%), DPC4 was retained, and no beta-catenin nuclear expression was found. **Invasive carcinoma:** Present in 14 cases (79%): 53% conventional tubular, 27% in situ-like with comedonecrosis, 13%, tubular-cystic, and 7% clear cell. Invasive component constituted 5-90% of the tumor (mean: 52%). **Outcome:** Follow-up information was available for 15 patients (83%) with a mean follow-up 48 mos (range 1-150). One patient with non-invasive disease died at 31 months. Two patients with invasive disease had perioperative mortality and were excluded from the analysis. No significant difference in survival (p=0.5) was found between non-invasive and invasive cases. Overall combined survival rates showed favorable prognosis:1yr 93%, 3yr 86%, 5yr 86%.

Conclusions: Biliary ITPNs show striking similarities to their pancreatic counterpart, both morphologically and immunophenotypically. Despite the relatively high incidence of invasive carcinoma (79%), biliary ITPNs, akin to the pancreatic ones, seem to have an indolent behavior significantly better than that of conventional adenocarcinomas (cholangiocarcinomas).

1756 Exome Sequencing Shows *BAP1* and *PBRM1* Are Recurring Somatic Mutations in Biphenotypic Liver Carcinoma

JK Sehn, WC Chapman, BR Tan, EM Brunt. Washington University, St. Louis, MO.

Background: Biphenotypic primary liver carcinoma (BPLC) with expression of both hepatocellular and biliary phenotypes is increasingly recognized as a distinct tumor type with worse prognosis than conventional hepatocellular carcinoma. These tumors often show immunohistochemical evidence of biphenotypic differentation within a seemingly homogenous epithelial tumor, making diagnosis of this tumor a challenge. The genetics of BPLC have not been evaluated, but next-generation sequencing (NGS) enables identification of malignancy-associated somatic mutations across all protein coding regions of the exome.

Design: Exome sequencing was performed on macrodissected FFPE tissue from 3 paired BPLC tumor and non-tumor liver samples, using 2x101-bp reads at 1000x coverage for the tumor samples. Single nucleotide variants (SNVs), insertions/deletions (indels), translocations, and copy number alterations (CNA) with at least 2.5% allele frequency (AF) were evaluated, and somatic status was confirmed for tumor mutations by comparison to paired non-tumor samples.

Results: Somatic SNVs and indels were identified in all 3 cases (23-63 variants/tumor); no structural variants or CNA were found. Two genes were recurrently mutated. The first recurrently mutated gene is *BAP1*, encoding a tumor suppressor. The second is *PBRM1*, encoding a SWI/SNF chromatin-remodelling complex component. Case 1 contained a 1-bp frameshift deletion (AF 16%) in *BAP1* and a 2-bp frameshift deletion (AF 15%) in *PBRM1*. Case 2 harbored a 1-bp frameshift insertion (AF 18%) in *BAP1* and a missense SNV (AF 15%) in *PBRM1*. Case 3 contained a *BAP1* missense SNV (AF 29%) and no *PBRM1* mutation. The likely pathogenic significance of these variants is suggested by recent studies defining a subset of *BAP1*--mutated clear cell renal cell carcinomas with worse cancer-specific survival compared to *BAP1* wild-type patients, with even shorter survival seen in patients with co-mutated *BAP1* and *PBRM1* tumors.

Conclusions: *BAP1* and *PBRM1* are recurrently somatically mutated in BPLC and may be involved in tumorigenesis and poor prognosis in this tumor type. The availability of immunohistochemical stains for *BAP1* suggests that evaluation of altered staining may be helpful in diagnosing this tumor type. Finally, pre-clinical studies evaluating targeted therapies for other *BAP1*-mutated tumors indicate that this recurring feature of BPLC may provide an avenue for direct therapy in this tumor type.

1757 Role of Serum Amyloid A in Advanced Alcoholic and Non-Alcoholic Steatohepatitis Compared to Other Etiologies of Chronic Liver Disease

M Shaar, Z McCroskey, R Chennuri, R Gamez, MM Picken, S Pambuccian, G Guzman. Loyola University Medical Center, Maywood, IL.

Background: Serum amyloid A (SAA) is an acute phase reactant expressed in hepatocytes in response to inflammation and many other stimuli; its overexpression is a well-established diagnostic feature of the inflammatory type hepatocellular adenoma. Recent studies suggested that higher expression is also seen in many neoplasms, including hepatocellular carciomas. Our aims were to study the expression of SAA in liver cirrhosis, to determine any correlation with the etiology of underlying disease.

Design: A tissue microarray was constructed from hepatectomy specimens of 109 patients with cirrhosis. Two 0.6 mm samples were obtained from each specimen. Standard immunohistochemistry using anti-SAA (mc1, Dako, 1:100 dilution) was employed on 4 micron sections. Blinded to clinical data, immunohistochemical expression of SAA was scored by microscopy as follows: 0-(<10% negative), 1-(10-25% weak), 2-(25-75% moderate) and 3-(>75% strong).

Results: Clinical data were obtained later, including the etiology of each case categorized as: Viral (72 patients, 66%: 63 HCV, 7 HBV and 2 both), NASH (12 patients, 11%), EtOH (10 patients, 9.2%) and Miscellaneous (15 patients, 13.8%). Miscellaneous cases included Wilson's disease, iron overload, autoimmune hepatitis, PBC and a1-antitrypsin deficiency. Cases were dichotomized into two categories: negative/low expression (scores 0 and 1) and moderate/strong expression (scores 2 and 3). Moderate/strong expression was seen in 91.67% of NASH cases and 90% of those caused by EtOH, compared to 54.17% and 66.67% in the viral and miscellaneous groups, respectively.

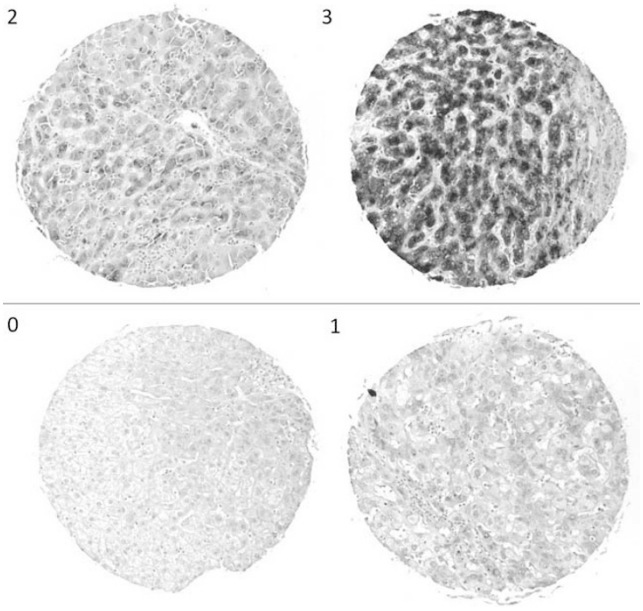

Statistical analysis using Fisher's Exact Test showed that NASH and EtOH cases have higher expression of SAA (moderate/strong) compared to the viral group (P=0.023 and 0.040, respectively). Results are similar when combined NASH and EtOH groups are compared to the viral group (P=0.0020), and to all other cases (P=0.0025).

Conclusions: SAA expression in hepatocytes was significantly higher in livers with advanced alcoholic and non-alcoholic steatohepatitis, compared to other etiologies of chronic liver disease. This result suggests that SAA may have an important role in the progression of chronic liver disease in alcoholic and non-alcoholic steatohepatitis.

1758 Astrocyte Elevated Gene 1 (AEG-1) May Be a Diagnostic Marker for Hepatocellular Carcinoma

M Sharma, B Ren, C Ryan, B Maliakkal, L McMahon, Q Yang, W Cao. University of Rochester Medical Center, Rochester, NY.

Background: Serum diagnostic markers have significantly improved early diagnosis and treatment of HCC. However, in certain situations such as in small biopsies, a biomarker will be helpful to assist in the diagnosis of HCC. Astrocyte elevated gene 1 (AEG-1), an oncoprotein, has been revealed in HCC animal models as a critical signaling molecule in tumor development, progression and metastasis. We evaluated AEG1 expression in human HCC, adjacent nonneoplastic liver and dysplastic nodule in resection specimens and correlated the AEG1 expression with clinical characteristics.

Design: A total of 52 tumor specimens from 36 patients were selected for this study. They included 43 HCCs with adjacent nonneoplastic liver tissue (38 cirrhotic and 5 non cirrhotic), and 9 dysplastic nodules. Sections were immunostained with anti-AEG1 antibody. The expression of AEG1 was evaluated with H-score method for both staining intensity (0-3) and percentage of positive cells. The mean value of the H-score of AEG1 in adjacent nonneoplastic liver, dysplastic nodule and HCC was analyzed by one-way analysis of variance.

Results: Diffuse and strong cytoplasmic AEG1 staining was found in HCC.

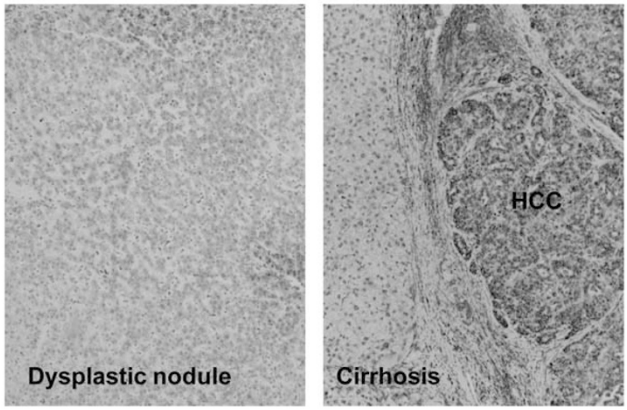

Compared to the adjacent nonneoplatic liver and dysplastic nodule, the mean H score of AEG1 in HCC (244.2±49.36) was significantly increased (P<0.0001). No significant difference of AEG1 expression was found between nonneoplatic liver and dysplastic nodule (mean H score125.7±46.5 and 122.8±33). High expression of AEG1 (H score≥200) was seen in 83% of HCC, compared to 0% in adjacent nonneoplatic liver and 0% in dysplastic nodule. In addition, the expression of AEG1 was not related to age, gender, tumor stage and recurrence/metastasis.

Conclusions: AEG1 is overexpressed in HCC. The high expression of AEG1 is exclusively seen in HCC lesions. The data suggests that AEG1 may be an ideal marker to discriminate HCC from benign lesions in difficult biopsy specimens.

1759 CPEB1, a Regulator of mRNA Translation, Is Associated with Poor Prognosis of Hepatocellular Carcinoma

M Sharma, B Ren, C Ryan, B Maliakkal, L McMahon, Q Yang, W Cao. University of Rochester Medical Center, Rochester, NY.

Background: Predicting prognosis of hepatocellular carcinoma (HCC) will greatly assist in deciding appropriate modality of therapy for HCC patients. No reliable biomarker is used clinically to predict HCC prognosis. Cytoplasmic polyadenylation element-binding protein 1(CPEB1), a dual-function protein that can repress and activate mRNA translation, may participate in cell proliferation and tumorigenesis. High level of CPEB1 mRNA has been reported in hepatic cancer cell line. We, for the first time, studied the expression of CPEB1 in human HCC specimens and correlated its expression with patient survival.

Design: 43 HCC resection specimens from 36 patients were selected for this study. Sections were immunostained with CPEB1 antibody. The expression of CPEB1 in HCC and adjacent nonneoplastic liver tissue (38 cirrhotic, 5 noncirrhotic) was evaluated with H-score method for both staining intensity (0-3) and percentage of positive cells. The mean value of the H-score of CPEB1 in HCC and nonneoplastic liver tissue was analyzed by one-way analysis of variance. Survival curve was calculated using the Kaplan–Meier method.

Results: There were 32 males and 4 females. The mean age of patients was 57.5 years (range, 23-73). Positive CPEB1 displayed cytoplasmic staining in hepatocytes. Compared to the adjacent non tumor areas, HCCs showed significant higher expression of CPEB1 (H-score, 141.7±52.18 vs 101.7±19.05, P<0.001). CPEB1 expression in HCC was independent of age, gender, tumor grade, stage and recurrence/metastasis. The patients with high expression of CPEB1 (H-score≥120) had a shorter survival compared to the ones with low CEBP1 expression.

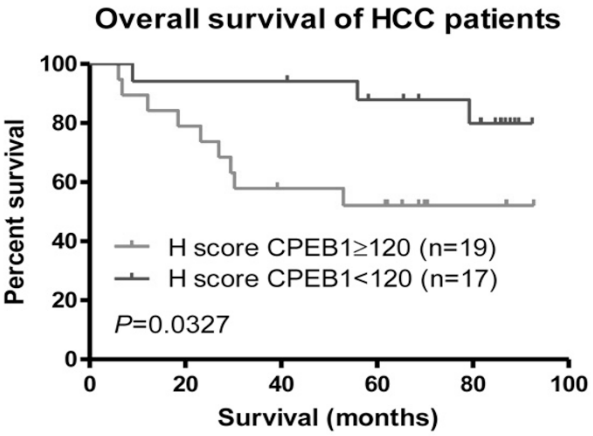

Conclusions: CPEB1 is overexpressed in HCC. The high CEBP1 expression in HCC may be an independent predictor for poor prognosis.

1760 Prognostic Implications of Isolated Central Perivenulitis as Initial Histologic Finding in Liver Transplant Patients: A Study with Sequential Biopsy Follow-Up

B Shetuni, S Rao, G-Y Yang. Northwestern University, Chicago, IL.

Background: In transplant liver biopsies, isolated central perivenulitis (ICP) as the initial histologic feature of rejection is an event with unclear implications.

Design: Of 400 liver transplants at our institution in last 4 years, we identified 9 cases with ICP as initial rejection feature and sequential biopsy follow-up. Banff working group guidelines were used for grading ICP and rejection with portal involvement..

Results: Average time to ICP was 153 days after transplant (12-365 days). ICP was defined as early onset (EO ICP; <100 days after transplant) or late onset (LO ICP; >100 days after transplant). Three patients had EO ICP (12-52 days) and 6 had LO ICP (116-365 days). ICP was graded as "minimal" (1), "mild" (6), and "moderate" (2). No further treatment was given after ICP finding. Subsequent biopsy follow-up revealed that all 3 EO ICP patients (two mild and one moderate ICP) showed progression to grade 3 acute rejection (183-350 days after ICP diagnosis), with two of them also showing bridging necrosis. In contrast, only two (33.3%) of 6 LO ICP patients (onset of ICP 116-165 days after transplant; one minimal and one mild ICP) had subsequent severe acute rejection, without bridging necrosis (p<0.05). No apparent association was found between progression to severe rejection and causes for transplant, which included hepatitis C, autoimmune hepatitis, alcohol and cryptogenic. Subsequent biopsies for the remaining 4 LO ICP patients showed that two had persistent ICP (120-418 days after initial ICP; initially one mild and one moderate ICP; on follow up both mild ICP) with no other histologic findings, and other two (mild to moderate ICP) displayed no ICP (120-355 days after initial ICP).

Conclusions: EO ICP is a significant harbinger of progression to severe acute rejection with variable necrosis. Additional immunosuppressive treatment to address EO ICP should be considered, although more cases are needed for definitive recommendation. Although risk of progression to severe acute rejection is lower in LO ICP, close follow-up is necessary as 33% of these patients did progress. ICP grade did not correlate with

development of severe acute rejection. Thus, even histologically underwhelming cases of ICP should be closely followed. No correlation was found between cause leading to transplant and development/timing of ICP in the transplanted liver.

1761 Under-Recognized Infiltrative and Plasma Cell-Poor Hepatitic Allo-Immune Liver Injury in Early Post-Transplant Period: Immediate and Long-Term Implications

I Siddiqui, N Selzner, S Hafezi-Bakhtiari, M Marquez, E Renner, SE Fischer, OA Adeyi. University Health Network, University of Toronto, Toronto, ON, Canada.

Background: Acute cellular rejection (ACR) post liver transplantation (LTX) is graded on the Banff scale of biliary epithelial, portal vein and hepatic vein endothelial cells injuries. Most ACR occur early post-LTX within the 1st year. A hepatitic plasma cell-rich variant is also recognized in later period and is relatively steroid-resistant. In this study we report two hitherto un-reported patterns of early ACR: sinusoidal infiltrative (iACR) and hepatitic (hACR), the latter having parenchymal inflammation/necrosis, ostensibly due to sinusoidal endothelial cells and hepatocellular allo-injuries. We describe their presentation and response to steroid boluses (SB) and compare these to typical moderate to severe ACR (tACR).

Design: Patients who had LTX from 2007 -2012 at the University Health Network, the largest transplant program in Canada, and who had biopsy-proven ACR in the 1st year were identified and corresponding liver biopsies reviewed. Patients with non-alloimmune hepatitis (e.g. HCV) were excluded. Transaminase (AST), alkaline phosphatase, and bilirubin at baseline, time of ACR, and followup were analyzed.

Results: Twenty eight biopsies from 27 patients were included; 15 /28 (53.6%) had tACR as described by the Banff criteria. Six (21.4%) had marked hepatitic inflammation (hACR) in addition to tACR features; and 7 (25.0%) had tACR plus prominent sinusoidal infiltration (iACR) by T-cells.

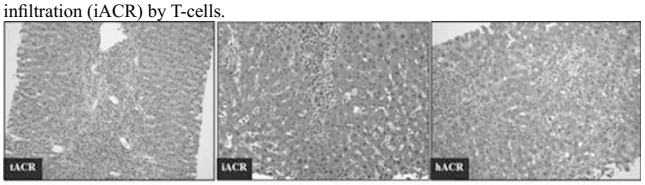

The iACR tends to occur later than the tACR (p=0.032) and had higher rise in AST compared to tACR, with mean ΔAST of 289 U/L versus 109 U/L (p = 0.046) for tACR; but only 1/7 (14.3% vs. 40% in tACR) failed SB and required thymoglobulin (TG). The hACR had similar ΔAST (p=0.12) but higher bilirubinemia than tACR (160 µmol/L vs. 35 mol/L; p= 0.039) and more often failed SB, requiring TG in 4/6 (66.7%) instances.

Conclusions: The iACR and hACR are currently poorly defined for grading. They occur in the first year with the iACR having higher ΔAST than tACR but responded to usual SB treatment better than tACR and hACR. The hACR is different from the better recognized plasma cell-rich late-occurring ACR in its pattern but shares its tendency for poor SB response.

1762 Fibrosis Progression in Hepatitis C Recurrence Post-Liver Transplantation Does Not Correlate with Ductular Reaction or Progenitor Cell Number at Time Zero Biopsy

A Trivedi, TD Schiano, S Ward, A Fenster, S Sclair, MI Fiel. Icahn School of Medicine at Mount Sinai, New York, NY; University of Miami, Miami, FL.

Background: Hepatitis C virus (HCV) RNA positive liver allograft recipients reinfect the allograft within hours after liver transplantation (LT) and frequently leads to chronic hepatitis and fibrosis in the allograft. A subset of patients develop advanced fibrosis within the first 2 years and are designated as rapid fibrosers. Ductular reaction and the activation of hepatic progenitor cells (HPCs) have been implicated in promoting liver fibrosis. The significance of donor liver characteristics in the later development of fibrosis has not been well studied and correlated with the subsequent development of fibrosis in the allograft. The aim of our study was to evaluate the pre/post-perfusion liver biopsies (time 0) for ductular reaction and HPC activation using immunohistochemical (IHC) stains for CK7, CK19 and EpCAM and correlate these findings with subsequent development of fibrosis.

Design: 10 patients who underwent LT for HCV were included in our study. All these patients had "time 0" and subsequent biopsies within 2 years of transplantation. Slides were graded and staged according to the Scheuer scheme. Patients with stage 0-2 were considered slow fibrosers while those with stage 3-4 were considered rapid fibrosers. IHC stains for CK7, CK19 and EpCam were performed on FFPE tissue for each biopsy. 5 portal tracts from each biopsy were evaluated for ductular reaction and number of HPCs using all three immunostains. The ductular reaction was scored as 1=limited to portal area, 2= extending into periportal zone and 3=extensive.

Results: The time 0 biopsies did not show any fibrosis. On subsequent post-LT biopsy, 5/10 (50%) patients had stage 0-1 fibrosis; 2/10 (20%) had stage 2 fibrosis; 2/10 (20%) had stage 3 fibrosis and 1/10 (10%) had stage 4 fibrosis. There was no significant difference in ductular reaction (p=0.64-0.89) or HPC number (p=0.45-0.62) of the time 0 biopsies between fast and slow fibrosers using any of the 3 immunostains.

Conclusions: We conclude that there is no correlation between the ductular reaction progenitor cell activation of the donor liver at time 0 on the subsequent development of fibrosis in the allograft. The interaction of the host and viral factors most likely play a larger role in the subsequent development of fibrosis.

1763 C4d Is Strongly Expressed in Portal Venules in Plasma Cell Hepatitis and May Be Used as a Diagnostic Marker and Predictor for Its Development

A Trivedi, TD Schiano, S Ward, J Levitsky, SN Thung, G Marina, M Fiel. The Mount Sinai Medical Center, New York, NY; Northwestern University Feinberg School of Medicine, Chicago, IL.

Background: Plasma cell hepatitis (PCH) is a severe form of post liver transplant (LT) allograft dysfunction and is considered a variant of rejection. In renal transplants, immunohistochemistry (IHC) for complement component 4d(C4d) is a reliable marker of antibody mediated rejection (AMR), however its role in post-LT allograft dysfunction is controversial. We hypothesize that PCH is a form of AMR. The purpose of our study is to investigate the C4d IHC staining pattern in patients with PCH.

Design: 17 post-LT hepatitis C (HCV) patients from 2 transplant centers that developed allograft dysfunction were included;11/17 had more than one liver biopsy;13/17 (76%) had PCH,2/17 (12%) developed severe recurrent HCV & 2/17 developed chronic rejection (CR). IHC for C4d (ARP, Waltham MA; 1:100 dilution) was performed on FFPE tissue. H&E slides were reviewed. For PCH,plasma cell (PC) scored based on number and ratio of PCs:0=none,1=occasional,2=10-30% (suggestive of PCH) and 3= >30% (consistent with PCH). C4d IHC staining was assessed by 2 liver pathologists blinded to the diagnosis and scored based on extent of staining:0=negative,1=<30%,2=30-75% and 3=>75% positive staining of portal venules (PV), central venules (CV) and sinusoids (S) present in the biopsy sample.

Results: 3+ C4d staining was consistently observed in PV as opposed to CV and S. Of 17 cases,13 (76%) cases had 3+ staining in PV;11/13 (85%) PCH cases had 3+ PV staining while 2/13 (15%) had 2+ PV staining. 9 of 13 PCH cases had liver biopsies prior to developing PCH and 5/9 (56%) had 3+, 2/9 (22%) had 2+, and 1/9 (11%) had 1+staining. Of 2 cases with recurrent HCV,1 showed 3+;the other had 1+ staining. Both these cases had a PC score of 2. Of the 2 CR cases 1 had 3+ and 1 had1+ PV staining. CV and S had 1+ staining in a minority of cases. Agreement between two pathologists was 100%.

Table 1: C4d staining intensity in PV

	3+	2+	1+
PCH (n=13)	11/13 (85%)	2/13 (15%)	0
Pre PCH biopsy (n=9)	5/9 (56%)	2/9 (22%)	1/9 (11%)
CR (n=2)	1/2 (50%)	0	1/2 (50%)
Severe recurrent HCV (n=2)	1/2 (50%)	0	1/2 (50%)

Conclusions: C4d staining in PVs is uniformly and strongly expressed in PCH and suggests that AMR may play a role in its development. Furthermore, our findings show that pre-PCH biopsies having moderate PC inflammation also had significant C4d staining and may predict the occurrence of PCH. Thus, the use of C4d IHC may play a role in the histological diagnosis of AMR induced PCH and thus allow for more timely and directed treatment.

1764 Chromogenic In Situ Hybridization for Albumin with Branch Chain Technology Is a Robust Marker of Hepatocellular Differentiation

JY Tse, A Mubeen, M Shahid, S Kakar, A Bateman, M Rivera, D Ting, V Deshpande. Massachusetts General Hospital, Boston, MA; University of California San Francisco, San Francisco; University Hospital Southampton NHS Foundation Trust, Southampton, United Kingdom.

Background: Albumin is widely recognized as a highly specific marker of hepatocellular carcinoma (HCC). However, its routine usage in the diagnostic laboratory has been hampered by the lack of a robust platform. We explore the utility of albumin detected by a branch chain chromogenic in situ hybridization (bISH) platform as a marker of hepatocellular differentiation, and compare its sensitivity with Hep Par 1 and Arginase-1. We also evaluate the specificity of albumin bISH.

Design: We evaluated 75 cases of HCC and 293 cases of non-hepatocellular neoplasms including adenocarcinomas of the lung (n=22), esophagus (n=40), stomach (n=72), colon (n=40), pancreas (n=95), endometrium (n=8), ovary (n=8), and urothelial carcinomas of the bladder (n=8). HCC cases included grade 1 (n=5), grade 2 (n=50), and grade 3 (n=20) tumors. The assays were performed on microarrays composed of 3 mm cores of tissue. We performed bISH for albumin and immunohistochemistry for Hep Par 1 and Arginase-1. Five previously uncharacterized hepatic neoplasms were also evaluated. Modified bISH probes were developed for albumin with QuantiGeneViewRNA technology (Affymetrix; Santa Clara, CA).

Results: Albumin bISH was positive in 74 cases of HCC with 72 cases showing positivity in greater than 50% of tumor cells. In contrast, 89.5% and 89.3% of HCCs were positive for Hep Par1 and Arginase-1, respectively. 75% and 51% of HCC showed reactivity in greater than 50% of cells for Hep Par 1 and Arginase-1, respectively. 100% of grade 1 HCC, 99% of grade 2 HCC and 100% of grade 3 HCC were positive for albumin bISH. 3 of the 5 previously uncharacterized neoplasms were positive for albumin bISH.

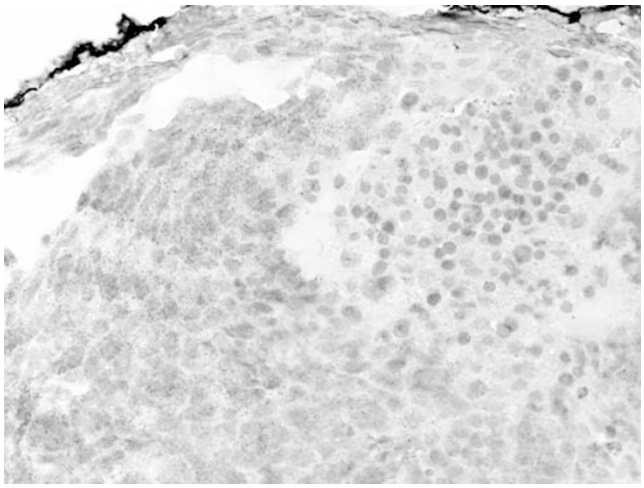

All non-hepatocellular neoplasms were negative for albumin.

Conclusions: bISH platform is a robust assay for detecting albumin and is superior to Arginase-1 and Hep Par 1 as marker of hepatocellular differentiation in terms of sensitivity and number of positive tumor cells. The increased sensitivity of this assay is not associated with a loss of specificity.

1765 The Utility of Routine HE Stain and Ubiquitin Immunohistochemistry in the Diagnosis of Steatohepatitis

SM Voss, CS Hollenbeak, Z Yang. Penn State Milton S. Hershey Medical Center, Hershey, PA.

Background: Ballooning degeneration (BD) is a key histologic feature in the diagnosis of steatohepatitis (SH), which represents a more aggressive form of fatty liver disease (FLD). Ubiquitin immunohistochemical stain has been shown to label hepatocytes with BD. We sought to compare routine HE with ubiquitin stain to determine the optimal number of cells with BD for the diagnosis of SH.

Design: A total of 149 adult (M:F=1, age range 20-79, median 52) liver biopsies with a diagnosis of FLD were retrieved from the anatomic pathology archive. HE slides were retrospectively reviewed to assess the percentage of steatosis and the greatest number of cells showing BD in a single high power field (HPF). Ubiquitin stain was performed and the greatest number of positive cells in a single HPF was similarly assessed. Four different cutoff values (≥1,≥5,≥10, and≥15/HPF) for cells with BD were used; the values were compared between HE and ubiquitin stains, and also to the original diagnosis. Association between BD on HE and ubiquitin stains was analyzed. The sensitivity and specificity of HE and ubiquitin were calculated for the diagnosis of SH.

Results: BD count on ubiquitin stain is significantly associated with BD on HE (ANOVA, $p<0.02$), but not with the degree of steatosis (ANOVA, $p>0.8$). Ubiquitin staining in the category of≥5 cells shows the best correlation with BD on HE (sensitivity 62%, specificity 93%, ROC area 0.804). In 67 cases without a diagnosis of SH, BD cell count on HE was 1.1±2.8/HPF (range 0-20, median 0) and ubiquitin-positive cell count was 3.7±9.1/HPF (0-60, median 0). In 82 cases with a diagnosis of SH, BD cell count on HE was 7.2±7.0/HPF (range 0-35, median 5) and ubiquitin-positive cell count was 15.5±15.8/HPF (range 0-60, median 15). On HE stain, BD≥1/HPF shows the best correlation with a diagnosis of SH, with a sensitivity of 93.9%, specificity of 71.6%, and ROC area 0.828. Ubiquitin-positive cells≥5/HPF shows the best correlation with the diagnosis of SH, with a sensitivity of 69.5%, specificity of 82.1%, and ROC area 0.758.

Conclusions: We confirmed the strong association between BD detected on HE and ubiquitin stain. In our study, for a diagnosis of SH the optimal number of cells with BD is≥1/HPF on HE or≥5 ubiquitin-positive cells/HPF. With the above cutoffs, HE stain is more sensitive while ubiquitin immunohistochemical stain is more specific.

1766 Hypomethylation of Long Interspersed Nuclear Element-1 Is Involved in the Early Tumorigenesis of Hepatocellular Carcinoma

W Wang, W Piao, H Zhang, L Jin, X Gao, J Qu, Z Xu, Y Yang, Z Piao. Ningxia People's Hospital, Yinchuan, China; Peking University People's Hospital, Beijing, China; The 302nd Hospital, Beijing, China; Kaiser Pernanente Fontana Medical Center, Fontana, CA.

Background: Hypomethylation of Long Interspersed Nuclear Element-1 (LINE-1) is consistently observed in many cancers including pancreatic, colonic, and stomachic carcinomas. In hepatocellular carcinoma (HCC), serum LINE-1 hypomethylation is reported to correlate with HBsAg status, large tumor size, and advanced tumor stage; therefore, it could be used as a poor prognostic marker for HCC. The aim of this study was to evaluate the role of the LINE-1 in the tumorigenesis of HCC.

Design: LINE-1 promoter methylation status was evaluated in 28 HCC by a methylation specific PCR (MSP) at CpG site 7 of LINE-1 promoter region (gene bank: X58075). In addition, fractional allelic losses (FAL) were measured in these tumors. To evaluate the actual value of FAL in each tumor, the microsatellite markers that showed a high frequency of loss of heterozygosity (LOH) in our previous studies were used, including D4S1545 (4q), D4S2920 (4q), D8S264 (8p), D8S1752 (8p), D16S498 (16q), D16S514 (16q), and p53 (17p). Finally, the association between the LINE-1 hypomethylation status and the clinicopathological parameters (HBV status, cirrhosis, tumor size, tumor differentiation, and FAL) was analyzed.

Results: Hypomethylation of LINE-1 was detected in 25 out of 28 HCCs (89%). The LINE-1 promoter was hypomethylated in 6 of 10 (60%) early HCCs (tumor size <3 cm) and 7 of 18 (41%) advanced HCCs (>3 cm). In addition, LINE-1 hypomethylation was detected in 5 of 15 (33%) well-differentiated and 8 of 13 (62%) poorly-differentiated tumors. To assess the association between hypomethylation status and FAL, the 28 tumors were divided into two groups according to the mean value of FAL (0.535): low (< 0.535) and high (> 0.535) FAL. Seven of 17 (54%) tumors with low FAL value showed hypomethylation, whereas 6 of 11 (46%) tumors with high FAL showed hypomethylation. No associations between hypomethylation of LINE-1 and HBV infection, age, sex, and cirrhosis were found.

Conclusions: The results strongly suggested that the hypomethylation of LINE-1 plays a role in the hepatocarcinogenesis; moreover, the hypomethylation of LINE-1 occurs not only in the progression of HCC, but also in the early stage of HCC tumorigenesis.

1767 Expression of Cathepsin K in Hepatic Angiomyolipoma

P Wang, D Cao. Beijing Ditan Hospital, Beijing, China; Peking University Cancer Hospital & Institute, Beijing, China.

Background: Cathepsin K is a lysosomal papain–like cystine proteinase that is commonly expressed in osteoclasts and activated macrophages. In macrophages Cathepsin K is under regulation by microphthalmia transcription factor. Recent studies have shown that cathepsin K is uncommonly expressed in epithelial tumors but is consistently present in renal angiomyolipomas. Although AML occurs most commonly in the kidney, it rarely occurs in the liver in which it often causes diagnostic confusion with hepatocellular carcinoma, especially in limited biopsy material. In this study we investigated the immunohistochemical profile of cathepsin K in a large series of 28 hepatic AMLs with comparison to HMB45, Melan-A and smooth muscle actin (SMA).

Design: Twenty-eight surgically resected hepatic AMLs were included for this study. One representative paraffin block from each case containing tumor and adjacent liver tissue was selected to generate 4 um unstained slides for immunohistochemical staining with anti-cathepsin K, HMB45, melan-A, and SMA. The staining was semi-quantitatively scored as 0 (<1% cells stained), 1+ (1-30%), 2+ (31-60%), 3+ (61-90%), and 4+ (>90%). The percentage of tumor cells stained for each marker was also recorded.

Results: Normal liver tissue was not stained with cathepsin K. All 28 hepatic AMLs showed positive staining for cathepsin K, including 3+ in 1 (4%) and 4+ in 27 (96%) cases. All AMLs showed positive staining for HMB45 including 1+ in 2 (7%), 2+ in 2 (7%), 3+ in 7 (25%) and 4+ in 17 (61%). All AMLs also showed positive staining for Melan-A [1+ in 9 (32%), 2+ in 4 (14%), 3+ in 12 (43%), and 4+ in 3 (11%)] and SMA [1+ in 7(25%), 2+ in 4 (14%), 3+ in 10 (36%), 4+ in 7(25%)]. The mean percentage of tumor cells stained with cathepsin K, HMB45, Melan-A and SMA was 97% (70-100%, median 100%), 81% (10-98%, median 90%), 52% (1-95%, median 50%), and 60% (10-100%, median 70%) , respectively ($p < 0.05$ for cathepsin K vs HMB45, $p<0.05$ for cathepsin K vs melan-A, $p <0.05$ for cathepsin K vs SMA).

Conclusions: Cathepsin K is highly expressed in all hepatic AMLs and is more sensitive than HMB45 and Melan-A for this tumor. Cathepsin K can be added in the diagnostic panel for hepatic AMLs, particularly in limited material.

1768 Erythropoietic Protoporphyria in Liver: A Clinicopathological Study of 6 Cases

SPS Yennam, FG Jalikis, PE Swanson, MM Yeh, MP Upton. University of Washington Medical Center, Seattle, WA.

Background: The porphyrias are disorders characterized by deficiency in the activity of enzymes involved in the biosynthesis of heme. In erythropoietic protoporphyria (EPP), a common mutation in ferrochelatase is associated with increased protoporphyrins in the liver. Up to 20% of EPP patients develop hepatobiliary disease, including acute liver failure and end-stage liver disease.

Design: 6 cases of hepatic EPP were identified from a single institution between 1991 and 2013. H&E and all available special stained slides, clinical records, and laboratory data were reviewed.

Results: 3 men and 3 women with a mean age of 44 years (range: 28-56) had been diagnosed with EPP at mean age 4.4 years (range: 2-9). Family history was positive in 1/6 cases, with one sibling affected. The mean laboratory findings included: total porphyrin 803 mcg/dl (range: 50-2070); protoporphyrin: 541 mcg/dl (range 318-786); ALT: 203 U/L (range: 34-575); AST: 162 U/L (range: 25-424); Alk Phos: 147 U/L (range: 66-313); total bilirubin: 5.4 mg/dl (range: 0.7-12.9). Histopathological findings include**:** pigment with "Maltese cross" birefringence (5 cases); cholestasis (5 cases); portal inflammation (6 cases); lobular inflammation (2 cases); fibrosis (6 cases), including advanced fibrosis (3 cases). 2 of 6 patients received liver transplant for liver failure and established cirrhosis; recurrent EPP occurred in each allograft liver (2 and 6 years after transplant, respectively). 2 of 6 patients died, 1 due to graft-versus-host disease after bone marrow transplantation, the other from intravenous catheter infection and sepsis.

Conclusions: Although uncommon, EPP should be in the differential diagnosis of liver failure. EPP may cause significant liver injury with potential for progressive fibrosis. Because liver transplant does not correct the constitutional ferrochelatase deficiency, recipients are at significant risk for recurrence. Close surveillance with frequent clinical and biochemical follow-up is warranted for patients after both primary diagnosis and after liver transplantation.

1769 Histological Sub Classification of Liver Cirrhosis with Laennec Staging System and Correlation with Clinical Findings

F Yilmaz, U Aykutlu, I Turan, M Orman, O Unalp, G Demirpolat, M Harman, Z Karasu, F Gunsar, D Nart, M Sozbilen, O Ozutemiz, U Akarca, G Ersoz, L Ferrell. University of Ege Faculty of Medicine, Izmir, Turkey; University of California San Francisco, San Francisco, Turkey.

Background: Histological diagnosis of cirrhosis is not adeaquate for clinical management since severity of cirrhosis is heterogeneous with different clinical stages. Laennec staging system (LSS) is a novel scoring system, subdividing the fibrosis stages of cirrhotic liver into 4A, 4B and 4C. This study aims to correlate the LSS scores, clinical and radiological parameters.

Design: Total hepatectomy specimens of 39 cases who underwent liver transplantation were retrospectively analyzed. LSS scoring was performed on Masson's trichrome stained sections of samples taken from the right lobe subcapsular region. Patients' data were collected from clinical files. Differences in demographic data, biochemistry prior to liver transplantation, Child-Pugh and MELD scores, Doppler Ultrasonography (DUSG) findings between patients with different LSS score subgroups were analyzed with Kruskall Wallis and Mann Whitney tests.

Results: There were 28 male, 11 male patients with a mean age of 53 (range, 26-64). The etiology of cirrhosis was viral (HBV, HBV+HDV, HCV) in 30 cases (77%), steatohepatitic (5 alcoholic and 1 non-alcoholic fatty liver disease) in 6 cases (15%) and mixed (HBV+alcohol) in 3 cases (8%). In 27 cases (69%) there was also HCC. LSS stages 3, 4A, 4B and 4C were 5%, 21%, 49% and 25%, respectively. There were no significant differences between the subgroups with respect to patient age and sex, body mass index, body weight, etiology , AST, albumin and globulin, DUSG findings. There was a tendency for increase in Child C frequency with higher stage of fibrosis (p=0, 06). In stage 4A, Child-Pugh and MELD scores, alkaline phosphatase, total and direct bilirubin levels were found to be significantly lower than stage 4C (p= 0,017, p= 0,047, p= 0,033, p= 0,017, respectively). Between stage 4A and 4B, ALT levels were significantly different (0,011). Total bilirubin was significantly different between stages 4A vs. 4B (p=0,044), 4A vs. 4C (p=0,033), and 4B vs. 4C (p=0,029).

Conclusions: LSS, which has been applied mainly on liver needle biopsy specimens up to date, seems to be capable of discriminating histological subgroups of liver cirrhosis with different clinical properties on total hepatectomy specimens as well.

1770 Immunostaining for CD34 in Sinusoidal Obstruction Syndrome Following Chemotherapy in Stem Cell Transplant

C Yoo, WS Twaddell. University of Maryland Medical Center, Baltimore, MD.

Background: Stem cell transplantation (SCT) is associated with numerous hepatic insults. Sinusoidal obstruction syndrome (SOS) is relatively common and severe cases carry a high mortality. The distinction from other cases of hepatic dysfunction is important, as many complications of SCT may result in liver injury with the specific diagnosis carrying considerable clinical significance. Despite the urgency of diagnosis, establishing SOS based on needle biopsy findings may be difficult as the characteristic features may be irregularly distributed. Many of the findings are those of large vein obstruction. Additionally, many patients are coagulopathic, and biopsies often consist of relatively small transjugular needle biopsies. CD34 is a cell-surface glycoprotein. Although immunostaining is usually positive in endothelial cells, this is not typically seen in hepatic sinusoids. It may be seen in abnormal sinusoids (e.g. in the setting of hepatocellular tumors). We investigate whether CD34 is overexpressed in sinusoids in SOS and may be a useful adjunct to diagnosis.

Design: 8 cases from June 2009 to September 2013 were selected. 4 cases were patients following ablative chemotherapy regimens and status-post SCT, diagnosed with SOS based on established morphologic criteria (sinusoidal dilatation and congestion, with occlusion of vessels by collagen). 4 other cases showed hepatic venous outflow obstruction (HVOO) with sinusoidal dilatation and congestion secondary to other causes such as cardiac failure. CD34 immunohistochemical stains were done and examined.

Results: 3 of 4 cases of SOS showed an increase in CD34 staining. 1 SOS case did not show an increase in CD34 staining. All 4 cases of HVOO due to other causes showed no increase in CD34 staining (p=0.04, N-1 two proportion test).

Conclusions: 3 cases of SOS showed increased staining for CD34; interestingly the exceptional case was showing clinical improvement at the time of biopsy, suggesting possible 'normalization' of the sinusoidal endothelium over time. In contrast, none of the cases of HVOO due to other cases showed increased staining. The difference between the two groups was statistically significant. The results suggest that CD34 staining, which is typically not seen in hepatic sinusoidal endothelium, is increasingly expressed in livers with SOS. This may represent a useful adjunct in establishing the critical diagnosis of SOS.

1771 Epithelial-Mesenchymal Transition Does Not Contribute to Fibrogenesis in Primary Sclerosing Cholangitis

L Zhao, R Ramachandran, S Liu, MD Hollenberg, Z Gao. University of Calgary, Calgary, AB, Canada; McGill University Health Center, Montreal, QC, Canada.

Background: Hepatic stellate cells (HSCs) play a central role in liver fibrogenesis but other cells have also been suggested to be a source of myofibroblasts. Biliary epithelial cells are thought to contribute to portal fibrogenesis via epithelial-mesenchymal transition (EMT) in chronic liver diseases including primary sclerosing cholangitis (PSC), mostly based on studies in cultured cholangiocytes showing expression of alpha-smooth muscle actin (αSMA). However such expression has not been demonstrated in vivo. These studies also showed focal double labeling of S100A4 and CK19 by immunohistochemistry. S100A4 was first identified in mice as a fibroblast specific protein (FSP1). Recent evidence however suggests that S100A4-positive cells in the liver do not express mesenchymal cell markers. The aim of this study was to investigate whether EMT contributes to fibrogenesis in primary sclerosing cholangitis.

Design: Formalin-fixed and paraffin-embedded sections from 49 liver biopsy and resection specimens (5 normal liver, 10 stage 1 PSC, 24 stage 2 PSC, 8 stage 3 PSC, 2 stage 4 PSC) were obtained for histological examination, immunohistochemistry, and immunofluorescence studies. Double labeling by immunohistochemistry with antibodies to S100A4 and CK19 was visualized with DAB and alkaline phosphatase. Immunofluorescence double staining with S100A4 and CK19, S100A4 and αSMA, S100A4 and CD68, as well as αSMA and CK19 was analyzed by confocal microscopy.

Results: Morphologically, S100A4-positive cells were inflammatory cells including macrophages and mononuclear cells. S100A4 did not stain HSCs or myofibroblasts. There was a significant increase in S100A4-positive cells in PSC compared to normal liver. Immunofluorescence double labeling showed no co-localization of S100A4 and αSMA, indicating that S100A4 is not a myofibroblast marker. A significant population of S100A4-positive cells was also positive for CD68, a macrophage marker. Epithelial cells of bile ducts and ductules were positive for CK19 but did not exhibit co-localization with S100A4. Myofibroblasts and a subpopulation of HSCs expressed αSMA but did not show CK19 immunoreactivity, indicating that bile duct cells are not transformed to mesenchymal cells in vivo.

Conclusions: We have demonstrated that cholangiocytes do not undergo EMT and do not contribute to fibrogenesis in PSC. Our data also indicated that S100A4 is not a fibroblast/myofibroblast marker.

1772 Segmental Cholangiectasia Clinically Worrisome for Intrahepatic Cholangiocarcinoma: Comparison with Recurrent Pyogenic Cholangitis (RPC)

L Zhao, M Hosseini, R Wilcox, Q Liu, T Crook, L Ferrell, J Hart. University Chicago, Chicago, IL; UCSF, San Francisco, CA; University Vermont, Burlington, VT; VA Dallas, Dallas, TX; Montefiore, New York, NY.

Background: This aim of this study was to review clinical, radiographic & pathologic features of cases of benign segmental cholangiectasia in non-Asian patients resected due to clinical concern for cholangiocarcinoma, and compare these features with cases of RPC in Asian patients.

Design: 12 patients underwent partial resection for segmental cholangiectasia due to cholangiographic findings of mural thickening and/or proximal biliary stricture worrisome for cholangiocarcinoma. Clinical & radiographic findings were obtained from medical records. H&E slides were reviewed & elastin stains & immunostains for IgG4, CD1a and Langerin were performed. 6 comparison cases of RPC in Asian patients were also examined.

Results: Age at dx (7 female, 5 male) ranged from 37 to 79 (median=67). No pt. had a hx of trauma or previous biliary surgery. One pt. was diagnosed by CT scan done for another reason. The others presented with abd. pain, wt. loss, jaundice, & elevated LFTs. 10 of 12 patients had cholangiectasia involving the left lobe only while 2 had both right & left lobe involvement. No patients had renal cysts, malnutrition or parasitic infection. Histologic examination revealed markedly dilated large intrahepatic bile ducts with mural fibrosis, periductal gland hyperplasia, and inflammation. Biliary dysplasia was not identified in any case. Hepatic parenchymal atrophy was evident in 8 pts & 5 had hepatolithiasis. Features reminiscent of ductal plate malformation were evident in the surrounding parenchyma in 6 cases. Elastic stains highlighted age-appropriate intimal fibrosis of large vessels adjacent to the cholangiectatic large ducts. IgG4 stains revealed no IgG4 associated sclerosing cholangitis. CD1a & Langerin stains highlighted Langerhans cells within the epithelium of the dilated large ducts, but no cells were present in the adjacent stroma. No gross or microscopic feature separated the Asian from non-Asian patients.

Conclusions: Although RPC is well described in Asian populations the dx is usually not considered in non-Asian U.S. patients. The etiology of this disorder in U.S. patients is unclear. It does not appear to represent a localized variant of Caroli's disease, hepatic Langerhans histiocytosis or IgG4 associated sclerosing cholangitis. The propensity for isolated left lobe involvement suggests relatively poor biliary drainage of the left ductal system compared to the right as a possible underlying factor.

1773 Centrilobular Ductular Reaction in NASH Correlates Well with Fibrosis Stage

L Zhao, M Westerhoff, J Hart. University of Chicago, Chicago, IL; University of Washington, Seattle, WA.

Background: There is increasing interest in the role of ductular reaction as part of the pathogenesis and characteristic histology of nonalcoholic steatohepatitis (NASH). However, earlier studies did not separately assess the contribution of portal and centrilobular ductular reactions over the spectrum of NASH. We herein report the utility of glutamine synthetase (GS) in conjunction with CK7 stains to separately delineate the character of the ductular reaction in each hepatic zone in biopsies with varying degrees of fibrosis.

Design: A total of 52 NASH biopsies were stained for CK7 and GS. The presence of CK7+ cells within each GS+ centrilobular zone (CLZ) of every biopsy was recorded as either: no CK7+ cells, isolated single CK7+ cells, CK7+ cells in strings, or CK7+ ductular structures. In addition every portal tract (PT) in the CK7 stained slides was graded as either: no ductular reaction, mild ductular reaction, or florid ductular reaction. The results were analyzed according to NASH stage.

Results: The prevalence and character of CK7+ cells in the CLZs (as identified by the GS stain) vary by NASH stage. In stage 0 cases there are rarely any CLZ CK7+ cells, and when present they are almost always in the form of isolated cells. As stage increases more CLZs contain CK7+ cells, and the prevalence of cells arranged as strings

or ductular structures also increases. In contrast, PT ductular reaction is present even in low stage biopsies and the degree of ductular reaction does not correlate well with stage.

	Centrilobular Zone				Portal Tracts		
	No CK7+ cells (%)	Single CK7+ cells (%)	Strings of CK7+ cells (%)	CK7+ ductules (%)	No ductular reaction (%)	Mild ductular reaction (%)	Florid ductular reaction (%)
Stage 0	82.6	17.1	0.4	0	33.0	52.8	14.1
Stage 1	73.2	20.9	3.0	3.0	26.3	52.9	20.8
Stage 2	54.2	23.2	14.3	8.3	23.2	62.1	15.3
Stage3	33.7	26.6	22.9	16.8	8.2	60.0	32.1
p value	<0.0001	0.54	0.0009	0.008	0.072	0.78	0.042

Conclusions: CK7+ CLZ ductular elements are common in NASH and their development correlates with increasing fibrosis stage. The presence of CLZ CK7+ ductular elements can cause confusion in distinguishing PTs from CLZs and GS stains can be helpful in this regard by highlighting CLZs. It is possible that the development of the CLZ ductular reaction contributes to the development of fibrosis in NASH. If so, scoring of CK7+ ductular elements would be a useful addition to the schema for GRADING in NASH.

1774 Abnormal Hepatocellular Mitochondria in Methylmalonic Acidemia

J Ziskin, Y Wilnai, G Enns, A-K Niemi, H Vogel. Stanford University, Palo Alto, CA.

Background: Methylmalonic acidemia (MMA) is one of the most frequently encountered forms of branched-chain organic acidemias. Biochemical abnormalities seen in some MMA patients, such as lactic acidemia and increased TCA cycle intermediate excretion, suggest mitochondrial dysfunction.

Design: In order to investigate the possibility of mitochondrial involvement in MMA, we examined the livers from patients with mutations that cause complete absence of methylmalonyl CoA mutase enzyme activity (MMA *mut^0*). .Biopsies from five explanted livers from MMA *mut^0* patients undergoing liver transplantation were evaluated for mitochondrial ultrastructural abnormalities. The patients ranged from 10 months to 17 years of age and all patients had previous episodes of metabolic acidosis, lactic acidemia, ketonuria and hyperammonemia.

Results: All biopsies revealed a striking mitochondriopathy by electron microscopy that were not found in control pediatric liver biopsies. Mitochondria were markedly variable in size, shape, and conformation of cristae. The inner matrix appeared to be greatly expanded and the cristae were diminutive and disconnected. No crystalloid inclusions were noted.

Conclusions: This study clearly documents extensive mitochondrial ultrastructure abnormalities in all liver samples in this series from MMA *mut^0* patients undergoing transplantation, providing pathological evidence for mitochondrial dysfunction in the pathophysiology of methylmalonyl CoA mutase enzyme inactivity. This series suggests that future studies are warranted in patients with alternative mutations in methylmalyonyl CoA mutase and patients with mutations in alternative genes associated with MMA, such as *MMAA*, *MMAB*, and *MMADHC* genes, in order to elucidate the prevalence and role of mitochondrial dysfunction across these diverse genetic causes. The marked enlargement of mitochondria in these cases may indicate a perturbation in mitochondrial fission in MMA. The correlation between mitochondrial dysfunction and morphological abnormalities in MMA may provide insights for better understanding and monitoring of optimized or novel therapeutic strategies.

Neuropathology

1775 Clinical Molecular Staging in Meningiomas: Prospective Experience of a Single Institution Using Routine FFPE Samples

MS Abedalthagafi, SH Ramkissoon, KL Ligon, AH Ligon, RD Folkerth, S Santagata. Brigham and Women's Hospital and Harvard Medical School, Boston, MA.

Background: Meningiomas are the most common primary intracranial tumors, and are clinically, histologically and molecularly heterogeneous. They are classified into the three World Health Organization grades: I (benign), II (atypical) and III (anaplastic). Several copy number variations (CNVs) have been suggested as prognostic factors, but real time molecular signatures using aCGH have never been used in routine clinical practice.

Design: We developed an array comparative genomic hybridization (aCGH) method to assess copy number changes in FFPE tissues (Craig JM., et al., PLoS One. 2012; 7(6):e38881). We performed aCGH on unselected 116 meningiomas received during a thirteenth-month period to test the hypothesis that different grades have different CNV signatures. Copy number aberrations were correlated further with clinical data.

Results: In addition to the known CNVs in the WHO classifications, we identified several new molecular signatures including: single copy loss in 12q , polysomy in chromosomes 3, 4, 5, 6, 7, 9, 13, 16, 18, 19, 20 and 21, occurring singly or in combination, in our sample. Three WHO grade I meningiomas with brain invasion, but insufficient WHO features of atypia, had grade II genomic signatures. Our genomic approach also led to the histologic re-classification of two uncertain "poorly differentiated neoplasms" into anaplastic meningioma.

WHO grade	22q- and/or 1p-	mono6 and/ or 6q-	Significant Others
I (n=65)*	36 (55.3 % of have 22q- , 27% have 22q- and 1p-)	6 (9.3%)	Trisomy 1,2,3,5,9,10,12,13,15,18,20,21 5(7.69%)
II (n=37)	25 (67.5%)	8(21.6%)	-3P,-19q, 1q+, monosomy 8trisomy 15 and 20 (18.9%)
III (n=14)**	7 (50%)	4 (28.5%)	19p+, trisomy 5 and 20, 9q-,17q- (21.4%)

* 3 cases had some but not all features of grade II, **2 cases had non-meningothelial tumors in differential.

Conclusions: The integration of histopathology with complex genetic/genomic data, results in the improved identification of clinically distinct meningioma subgroups, which in turn directs the clinical care plan for certain patients. Such results will also facilitate the development of targeted therapeutic strategies.

1776 The Genomic Copy Number Profile of Angiomatous Meningioma

MS Abedalthagafi, SH Ramkissoon, KL Ligon, AH Ligon, RD Folkerth, S Santagata. Brigham and Women's Hospital and Harvard Medical School, Boston, MA.

Background: Angiomatous meningioma is an uncommon World Health Organization (WHO) grade I subtype of meningioma. It has numerous small or large vascular channels which may predominate over the meningothelial elements, often making the diagnosis challenging. We present here novel genomic copy number signatures of three cases of angiomatous meningioma.

Design: We studied three cases of angiomatous meningioma (from two females and one male). The mean age of the patients is 75 years. Array-based comparative genomic hybridization (aCGH) was performed using the stock 1x1M Agilent SurePrint G3 Human CGH Microarray chip to identify tumor-specific genomic copy number changes in FFPE clinical samples (Craig JM., et al., PLoS One. 2012; 7(6):e38881).

Results: aCGH revealed polysomy (i.e., more than two copies) of several chromosomes including: 5, 6, 7, 12, 13, 15, 16, 17, 18, 19, 20, 21, and 22. Interestingly, the common genomic variants in type I meningioma, like monosomy 22 or 1p loss or neutral copy number changes, were not observed in angiomatous meningioma.

Conclusions: Angiomatous meningiomas generally share histologic, prognostic and clinical features of other WHO grade I meningiomas. Data from our three cases suggests that this meningioma subtype might have a unique genomic copy number profile. Because the angiomatous subtype can sometimes pose diagnostic difficulty to pathologists due to confusion with other vascular meningeal lesions the presence of chromosomal trisomies might be of significant diagnostic utility. Moreover, our findings might help elucidate the pathogenesis of these tumors. Evaluation of additional tumors of this subtype is now needed.

1777 High Expression of Olig2 Is Restricted to Gliomas and Is More Common in Oligodendrogliomas Than Astrocytomas

CL Appin, C Cohen. Emory University School of Medicine, Atlanta, GA.

Background: Olig2, a bHLH transcription factor, is restricted to oligodendroglial differentiation in normal human brain, but has been found to be expressed in both oligodendrogliomas and astrocytomas of different grades. As such, this marker is not useful in differentiating an oligodendroglioma from an astrocytoma but is used to distinguish a glioma from other central nervous system (CNS) and non-CNS malignancies. Results from studies assessing Olig2 expression are mixed, with some finding stronger expression in oligodendrogliomas compared to astrocytomas while others show equal expression in the two groups. Additionally, Olig2 expression has been found in other CNS as well as non-CNS tumors. The purpose of this study was to assess Olig2 expression in oligodendrogliomas, astrocytomas and various non-CNS tumors.

Design: Tissue microarrays (TMAs) of glioblastoma (GBM) tumors (n=27) and anaplastic astrocytomas (n=21) as well as individual cases of oligodendrogliomas (n=20) were assessed for Olig2 expression. A TMA of non-CNS tissue (both malignant and normal), including tonsil, breast, placenta, prostate, colon, thyroid, skin, pancreas, ovary, mesothelium, testis, thymus, liver, spleen, and salivary gland, was also stained for Olig2. Also included were cerebral cortex and pituitary gland (one case each). Each tumor was assigned an intensity (1+ to 3+) and the percentage of cells staining was determined. The intensity and percentage of cells staining for each tumor was multiplied to give a q-score (0 to 300). Statistical analysis was performed using the Wilcoxon rank-sum test.

Results: Oligodendrogliomas showed significantly higher expression of Olig2 compared to other gliomas combined ($p < 0.001$). Gliomas as a whole likewise showed significantly higher Olig2 expression compared to non-CNS tumors ($p < 0.001$). Intensity of staining in gliomas ranged from 0-3+ while that of non-CNS tumors ranged from 0-1+.

Conclusions: High expression of Olig2 is seen only in gliomas, although faint immunoreactivity is present in some non-CNS tumors. Oligodendrogliomas show stronger immunoreactivity compared to astrocytomas.

1778 Meningiomas That Meet Grade II by 3 Criteria Have an Increased Rate of Recurrence

CL Appin, SG Neill, RH Press, RS Prabhu, I Crocker, DJ Brat. Emory University School of Medicine, Atlanta, GA.

Background: Meningiomas are graded according to the World Health Organization (WHO) criteria as grade I, II or III. While grade I meningiomas are considered benign, grade II and III tumors recur more frequently and have a worse prognosis. Criteria for classification as grade II include 1) brain invasion; 2) specific histologic patterns (chordoid and clear cell); 3) increased mitoses; and 4) the presence of at least 3 of 5 atypical features (increased cellularity, sheet-like growth, prominent nucleoli, 'spontaneous' or 'geographic' necrosis and small cells with a high nuclear to cytoplasmic ratio). The purpose of this study was to determine whether meningiomas that meet more than one criterion for grade II are more aggressive than those that meet only one criterion.

Design: Seventy-one grade II meningiomas resected at Emory University Hospitals from 2000-2010 were included. Slides, pathology reports, and patient charts from each case were reviewed. Meningiomas were grouped according to number of histopathologic criteria met to establish a grade II diagnosis and correlated with time to recurrence and survival data. Median follow-up time was 3.2 years. Statistical analysis was performed using Fisher's exact test and SAS-JMP software.

Results: Meningiomas that met 3 criteria (n=7) for classification as a grade II neoplasm had a higher recurrence rate (85.7%) than those that only met one (n=39) or two (n=23) criteria (33.3%; p=0.0146 and 26.1%; p=0.0086, respectively). No significant difference